AD_____

Award Number: DAMD17-99-1-9515

TITLE: Determining Gene Expression, Substrate Specificity and Natural Substrates for Prostate Associated Proteases

PRINCIPAL INVESTIGATOR: Toshihiko Takeuchi, Ph.D.

CONTRACTING ORGANIZATION: University of California, San Francisco
San Francisco, California 94143-0962

REPORT DATE: July 2001

TYPE OF REPORT: Annual Summary

PREPARED FOR: U.S. Army Medical Research and Materiel Command
Fort Detrick, Maryland 21702-5012

REPORT DOCUMENTATION PAGE

Form Approved
OMB No. 074-0188

1. AGENCY USE ONLY (Leave blank)	2. REPORT DATE	3. REPORT TYPE AND DATES COVERED
	July 2001	Annual Summary (1 Jul 00 - 30 Jun 01)

4. TITLE AND SUBTITLE

Determining Gene Expression, Substrate Specificity and Natural Substrates for Prostate Associated Proteases

5. FUNDING NUMBERS

DAMD17-99-1-9515

6. AUTHOR(S)

Toshihiko Takeuchi, Ph.D.

7. PERFORMING ORGANIZATION NAME(S) AND ADDRESS(ES)

University of California, San Francisco
San Francisco, California 94143-0962
E-Mail: toshi@foxtrot.ucsf.edu

8. PERFORMING ORGANIZATION REPORT NUMBER

9. SPONSORING / MONITORING AGENCY NAME(S) AND ADDRESS(ES)

U.S. Army Medical Research and Materiel Command
Fort Detrick, Maryland 21702-5012

10. SPONSORING / MONITORING AGENCY REPORT NUMBER

11. SUPPLEMENTARY NOTES

Report contains color

12a. DISTRIBUTION / AVAILABILITY STATEMENT

Approved for Public Release; Distribution Unlimited

12b. DISTRIBUTION CODE

13. ABSTRACT *(Maximum 200 Words)*

14. SUBJECT TERMS

Gene Expression, Prostate Associated Proteases

15. NUMBER OF PAGES

26

16. PRICE CODE

17. SECURITY CLASSIFICATION OF REPORT	18. SECURITY CLASSIFICATION OF THIS PAGE	19. SECURITY CLASSIFICATION OF ABSTRACT	20. LIMITATION OF ABSTRACT
Unclassified	Unclassified	Unclassified	Unlimited

Table of Contents

INTRODUCTION

Numerous studies have shown that proteolytic enzymes play an essential role in tumor invasion, metastasis and angiogenesis (1,2, 3). Proteases may enhance these processes through the release and/or activation of growth factors and the degradation of extracellular matrix. Thus, inhibition of these protease-mediated processes may be a therapeutic strategy for the treatment of metastatic cancer. Indeed, proteases, in general, have proven to be excellent chemotherapeutic targets as evidenced by the HIV protease inhibitors and the large number of successful clinical trials involving protease inhibitors (4). This proposal focused upon serine proteases of the chymotrypsin fold due to the wealth of information that exists on structure-function relationships regarding this class of enzymes and the existence of potent and specific inhibitors that are readily available for their inhibition. In addition, understanding of the function of these proteases may lead to further insight into cancer biology and may lead to possible therapeutics. In particular, we proposed to understand serine protease function by identifying serine protease substrates and substrate specificity. These techniques used and developed should become increasingly useful as the Human Genome Project continues to provide numerous serine protease genes whose products have no known function. These studies should be generalizable to other classes of proteases and to other enzymes such as kinases. In addition, perhaps a greater understanding of prostate and prostate cancer biology can be gained by examining the interaction of the proteases and downstream substrates within a tumor tissue and during various stages of cancer.

BODY

We recently reported the cloning and initial characterization of membrane-type serine protease 1 (MT-SP1) from the PC-3 human prostatic cancer cell line (5).We have found subcutaneous coinjection of PC-3 cells with wild-type ecotin or ecotin M84R/M85R led to a decrease in the primary tumor size compared to animals in whom PC-3 cells and saline were injected (Melnyk et al, unpublished results). Since both wild-type ecotin and ecotin M84R/M85R are potent, subnanomolar inhibitors of MT-SP1, these studies raise the possibility that MT-SP1 plays an important role in progression of epithelial cancers expressing this protease.Northern blotting showed that MT-SP1 was strongly expressed in the gastrointestinal tract and the prostate, while lower expression levels were observed in the kidney, liver, lung, and spleen. The function of MT-SP1 and its possible role in pathological states is still undetermined. However, potent macromolecular inhibitors of MT-SP1 have been identified and reagent quantities of a His-tagged fusion of the MT-SP1 protease domain were expressed in *E. coli*, purified and autoactivated (5).

The substrate specificity of MT-SP1 was determined using a positional scanning-synthetic combinatorial library and substrate phage techniques. The specificity was found to be: (P4 = K>R; P3 = R/K/Q; P2 = S>F/G). Protease-activated receptor 2 (PAR2) and single-chain urokinase-type plasminogen activator are proteins that are localized to the extracellular surface and contain the preferred MT-SP1 cleavage sequence. The ability of MT-SP1 to activate PARs was assessed by exposing PAR-expressing Xenopus oocytes to

the soluble MT-SP1 protease domain. The latter triggered calcium signaling in PAR2-expressing oocytes at 10 nM but failed to trigger calcium signaling in oocytes expressing PAR1, PAR3, or PAR4 at 100 nM. Single-chain urokinase-type plasminogen activator was activated using catalytic amounts of MT-SP1 (1 nM), but plasminogen was not cleaved under similar conditions. The membrane localization of MT-SP1 and its affinity for these key extracellular substrates suggests a role of the proteolytic activity in key regulatory events. These data concerning the substrate specificity of MT-SP1 was published in The Journal of Biological Chemistry (6).

Task 1. Determine *in vitro* substrate specificity for MT-SP1 and MT-SP2 using a positional scanning-synthetic combinatorial library and substrate phage display (months 1-9).

A. Assay *in vitro* substrate specificity for MT-SP1 and MT-SP2 using positional scanning library
B. Synthesize and purify small molecule synthetic substrates for MT-SP1 and MT-SP2, and characterize protease activity against substrates.
C. Design, create, and screen substrate phage display library.

Tasks 1A-1C were completed for MT-SP1 and published in The Journal of Biological Chemistry, as described above (6). During the second funding period, effort was made for the expression and characterization of MT-SP2. MT-SP2 was produced in a baculovirus system in a His-tagged form. Rabbit polyclonal antibodies against MT-SP2 derived from *E. coli* expressed antigen were used to verify expression and purification from baculovirus.

Levels of MT-SP2 were too low to assay in the positional scanning library. However, activation of MT-SP2 was observed upon treatment of 1 nM MT-SP1. Therefore, in vitro, MT-SP2 is an excellent substrate for MT-SP1 as predicted upon examination of the activation sequence of MT-SP2 compared with the cleavage specificity of MT-SP1.

Task 2. Generate a human prostate cDNA library for use in the identification of natural substrates for MT-SP1 and MT-SP2 using small pool cDNA expression cleavage screening (months 10-17).

A. Generate and characterize human prostate cDNA library.
B. Screen cDNA library using expression cleavage screening.
C. Isolate and characterize clones derived from screen.

Since Task 1 was completed with MT-SP1, the next phase of the project is to identify possible natural substrates. We initially proposed to use small pool cDNA expression cleavage screening in Task 2; however, there was enough information from the substrate specificity data derived from Task 1 to choose logical candidate substrates for MT-SP1 without using the small pool cDNA expression cleavage screening.

Therefore, we successfully used a candidate approach for the identification of macromolecular substrates of MT-SP1.

We have previously shown that Protease Activated Receptor 2 (PAR-2) and single-chain uPA are excellent in vitro substrates for MT-SP1 (6). Baculovirus expressed MT-SP2 was also activated using low levels (1 nM) of MT-SP1. These studies validate the candidate approach where the protease specificity is determined, and then this substrate specificity is used to identify likely candidates for cleavage and activation.

Task 3 was proposed for months 18-24; my tenure at UCSF was terminated in month 15 of the proposal and was not completed.

Key Research Accomplishments

- Assayed *in vitro* substrate specificity for MT-SP1 using positional scanning library
- Synthesized and purified small molecule synthetic substrates for MT-SP1 and MT-SP2, and characterized protease activity against substrates.
- Designed, created, and screened two substrate phage display libraries against MT-SP1
- The preferred cleavage sequences for MT-SP1 were found to be {P4-(Arg/Lys) P3-(X) P2-(Ser) P1-(Arg) P1'-(Ala)} and {P4-(X) P3-(Arg/Lys) P2-(Ser) P1(Arg) P1'(Ala)} where X is a non-basic amino acid.
- Using the preferred substrate cleavages, macromolecular substrates for MT-SP1 were identified:
  - –10 nM soluble MT-SP1 protein activates protease activated receptor-2 (PAR2) but not PAR1, PAR3, or PAR4.
  - –1 nM soluble MT-SP1 protein activates single-chain urokinase type plasminogen activator, but not plasminogen.
  - -1 nM soluble MT-SP1 protein activates MT-SP2.

–The membrane localization of MT-SP1 and its affinity for these key extracellular substrates suggests a role of the proteolytic activity in regulatory events.

Reportable Outcomes

Paper:

T. Takeuchi, J. L. Harris, W. Huang, K. W. Yan, S. R. Coughlin, and C. S. Craik " Cellular localization of membrane-type serine protease 1 and identification of protease activated receptor-2 and single-chain urokinase-type plasminogen activator as substrates ", *J. Biol. Chem* **275**, 26333-26342 (2000).

Selvarajan, S., Lund, L. R., Takeuchi, T., Craik, C. S., and Werb, Z. " A plasma kallikrein-dependent plasminogen cascade required for adipocyte differentiation", *Nat. Cell Bio.* 3, 267-275 (2001)

Talk:

T. Takeuchi, J. L. Harris, F. Elfman , W. Huang, K. Yan, S. R. Coughlin, M. A. Shuman, and C. S. Craik "Using Macromolecular Protease Inhibitors to Dissect Complex Biological Processes: Identification and Characterization of a Membrane-Type Serine Protease in Epithelial Cancer and Normal Tissue", International Symposium on Proteases: Basic Aspects and Clinical Relevance, Montebello, Quebec, 2000.

Employment:
Upon completion of my work at UCSF, I obtained employment at Bayer Corp. in Berkeley, California as a senior research scientist.

References

1. Aznavoorian, S., Murphy, A. N., Stetler-Stevenson, W. G., and Liotta, L. A. (1993) "Molecular aspects of tumor cell invasion and metastasis." *Cancer* **71,** 1368-1383.
2. Chen, W. T. (1992) "Membrane proteases: roles in tissue remodeling and tumor invasion." *Curr. Opin. Cell Biol.* **4,** 802-809.
3. Liotta, L. A., Steeg, P. S., and Stetler-Stevenson, W. G. (1991) "Cancer metastasis and angiogenesis: an imbalance of positive and negative regulation." *Cell* **64,** 327-336.
4. Deeks S. G., Smith M., Holodniy M., Kahn, J. O. (1997) HIV-1 protease inhibitors. A review for clinicians.
Jama, **277,** 145-53
5. Takeuchi, T., Shuman, M. A., and Craik, C. S. (1999) *Proc. Natl. Acad. Sci. USA* **96,** 11054-11061
6. Takeuchi, T., Harris, J. L., Huang, W., Yan, K. W., Coughlin, S. R., and Craik, C. S. (2000) *J. Biol. Chem.* **275,** 26333-26342

A plasma kallikrein-dependent plasminogen cascade required for adipocyte differentiation

Sushma Selvarajan*†, Leif R. Lund†‡, Toshihiko Takeuchi†, Charles S. Craik† and Zena Werb*§

*Department of Anatomy, Box 0452, and †Department of Pharmaceutical Chemistry, Box 0446, University of California, 513 Parnasssus Avenue, San Francisco, California 94143, USA

‡Finsen Laboratory, Copenhagen University Hospital, Strandboulevarden 49, DK-2100 Copenhagen, Denmark

§e-mail: zena@itsa.ucsf.edu

Here we show that plasma kallikrein (PKal) mediates a plasminogen (Plg) cascade in adipocyte differentiation. Ecotin, an inhibitor of serine proteases, inhibits cell-shape change, adipocyte-specific gene expression, and lipid accumulation during adipogenesis in culture. Deficiency of Plg, but not of urokinase or tissue-type plasminogen activator, suppresses adipogenesis during differentiation of 3T3-L1 cells and mammary-gland involution. PKal, which is inhibited by ecotin, is required for adipose conversion, Plg activation and 3T3-L1 differentiation. Human plasma lacking PKal does not support differentiation of 3T3-L1 cells. PKal is therefore a physiological regulator that acts in the Plg cascade during adipogenesis. We propose that the Plg cascade fosters adipocyte differentiation by degradation of the fibronectin-rich preadipocyte stromal matrix.

Adipogenesis is regulated by hormones such as leptin[1] and by transcription factors such as peroxisome-proliferator-activated receptor-γ (PPARγ)[2]. However, it is not generally appreciated that, during adipocyte differentiation, the fibronectin-rich stromal matrix of preadipocytes is converted to the basement membrane of adipocytes[3]. Thus, although some of the intracellular events that occur during adipocyte differentiation are know understood[4], the role of the extracellular matrix (ECM) is yet to be explored. Here we investigate the hypothesis that ECM-degrading proteases are required during adipogenesis. We focus on the Plg system of serine proteases, as plasmin directly cleaves various ECM molecules, including fibronectin[5] and laminin[6], and releases bound cytokines such as insulin-like growth factor I (IGF-I)[7]. Plg can be activated (converted to plasmin) by urokinase-type plasminogen activator (uPA) and by tissue-type plasminogen activator (tPA). Here we report the use of genetic and inhibitor-based approaches to evaluate the role of serine proteases during both adipogenic differentiation of preadipocytes in culture and repopulation of adipocytes during involution of the murine mammary gland *in vivo*. Our results demonstrate an important function of the Plg system of serine proteases during adipocyte differentiation.

Results

Inhibition of serine proteases reduces differentiation of 3T3-L1 cells. To identify the serine proteases in the plasminogen cascade that function during adipocyte differentiation, we used a new inhibitor-based approach to block their activity during differentiation of 3T3-L1 cells. Ecotin is a macromolecular inhibitor that inhibits a broad range of chymotrypsin-like serine proteases such as trypsin, chymotrypsin and elastase[8]. Wild-type (WT) ecotin is a poor inhibitor of uPA and plasmin; however, the ecotin mutant MM84,85RR (EcoRR) is a nanomolar inhibitor of uPA[9]. Addition of WT ecotin or EcoRR had no effect on preadipocytes, but reduced adipose conversion to <20% of control levels (Fig. 1a, b). Three lines of evidence indicate that the lack of lipid accumulation was a result of blockage of the differentiation pathway. First, most ecotin-treated cells failed to undergo morphologic differentiation (rounding up). Second, CCAAT/enhancer-binding protein-β (C/EBPβ; Fig. 1c) and PPARγ (Fig. 1d), both of which are required for adipogenic differentiation[2,10], were only weakly expressed in ecotin-treated cells. Third, levels of glycerophosphate dehydrogenase (GPDH), an enzymatic marker for differentiated adipocytes[11], were only ~20% of control levels in cells cultured with either form of ecotin (data not shown). These data support a functional role for serine proteases during differentiation of predipocytes in culture.

To analyse further the functions of plasminogen and plasminogen activators, we treated 3T3-L1 cells with the serpin proteins α-2-antiplasmin (α2-AP, which inhibits plasmin[12]) and plasminogen-activator inhibitor-1 (PAI-1, which inhibits uPA and tPA[13]), and monitored their differentiation. Our data support the hypothesis that plasmin is required during differentiation of 3T3-L1 preadipocytes in culture. Treatment of cells with α2-AP during differentiation inhibited adipose conversion and lipid accumulation (Fig. 1h, i). On the other hand, uPA and tPA do not seem to be required for adipogenesis, as treatment with PAI-1 had no effect on 3T3-L1 differentiation (Fig. 1g, i).

Adipogenic differentiation of 3T3-L1 cells is Plg-dependent. We analysed the expression of uPA and tPA in both preadipocytes and differentiated adipocytes. We detected uPA and tPA in both the conditioned medium and cell lysates of 3T3-L1 preadipocytes (Fig. 2a). Two other caseinolytic serine proteases, with relative molecular masses of 80,000 (M_r 80K) and 120K (termed sp80 and sp120, respectively), were present in the conditioned media of both 3T3-L1 preadipocytes and differentiated adipocytes; these proteases were inhibited by phenylmethylsulfonyl fluoride (PMSF). An activity similar to sp80 was also present in fetal bovine serum (FBS). Expression of uPA and tPA decreased with adipogenic differentiation. These data raise the question of how Plg functions during adipogenesis. Preadipocytes grew normally in 10% FBS that was depleted of Plg (Fig. 2b). However, once cells were induced to differentiate, they exhibited <10% adipose conversion relative to cells cultured in complete FBS (Fig. 2c, d). Addition of exogenous Plg to Plg-depleted FBS rescued differentiation (Fig. 2e). Preadipocytes differentiated into adipocytes in normal human plasma, albeit to a lesser extent than in FBS (see later). However, no adipose conversion or lipid accumulation was seen in cells that were induced to undergo differentiation in Plg-deficient human plasma. Addition

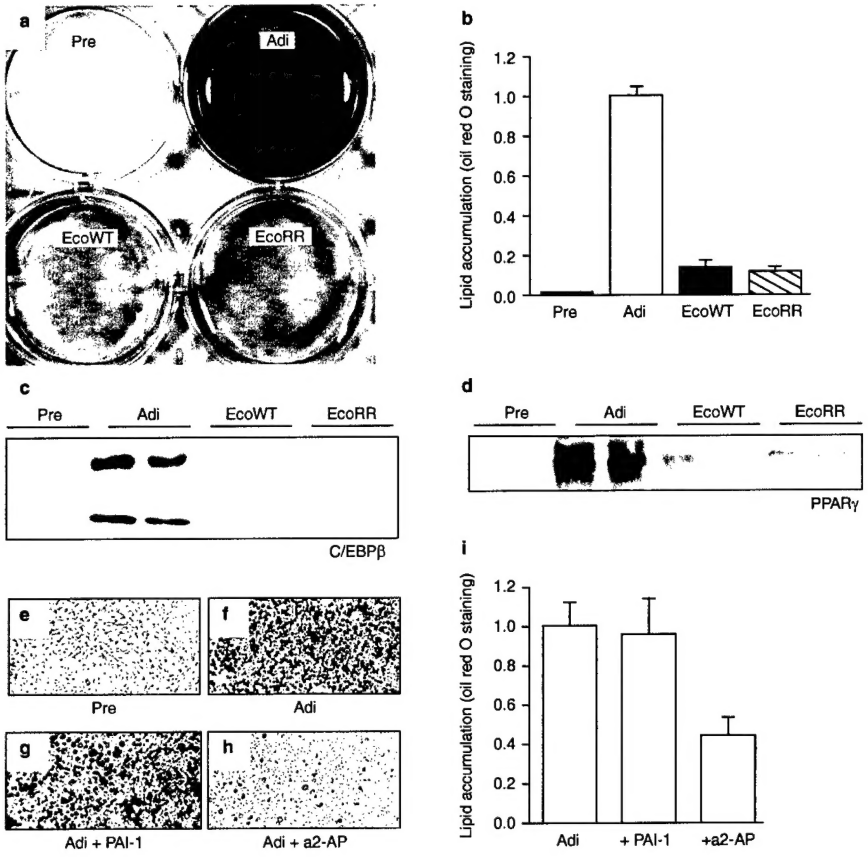

Figure 1 **Inhibition of serine proteases during differentiation of 3T3-L1 cells reduces adipose conversion. a**, **e–h**, Staining of cells with Oil red O to visualize the extent of adipose conversion. **b**, **i**, Quantification of lipid accumulation; absorbance is designated as 1.0 for adipocytes. Data are means ± s.d. **c**, **d**, Western blotting of 3T3-L1 nuclear lysates to detect C/EBPβ (**c**) and PPARγ (**d**). Pre, 3T3-L1 preadipocytes; Adi, adipocytes, EcoWT, differentiating cells treated with WT ecotin; EcoRR, differentiating cells treated with EcoRR. Where indicated, adipocytes were treated with PAI-1 or α-2-antiplasmin (α2-AP).

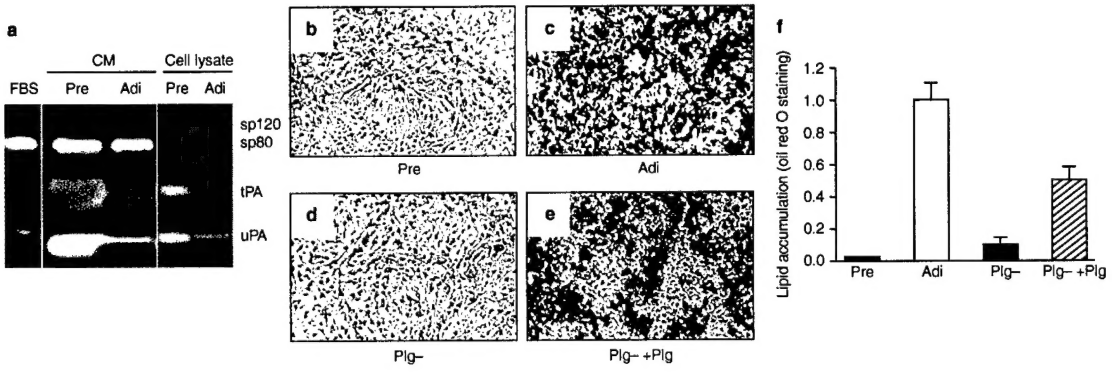

Figure 2 **The Plg system is regulated and required during 3T3-L1 cell differentiation. a–e**, Staining with Oil red O to detect adipocytes. **a**, Casein/Plg zymograms. FBS, fetal bovine serum; CM, conditioned medium; Pre, 3T3-L1 preadipocytes; Adi, adipocytes. **b**, Preadipocytes grown in Plg-depleted serum. **c**, Cells differentiated in normal serum. **d**, Cells differentiated in Plg-depleted serum. **e**, Cells differentiated in Plg-depleted serum with exogenous Plg added. **f**, Quantification of adipose conversion; absorbance is designated as 1.0 for adipocytes. Data are means ± s.d.

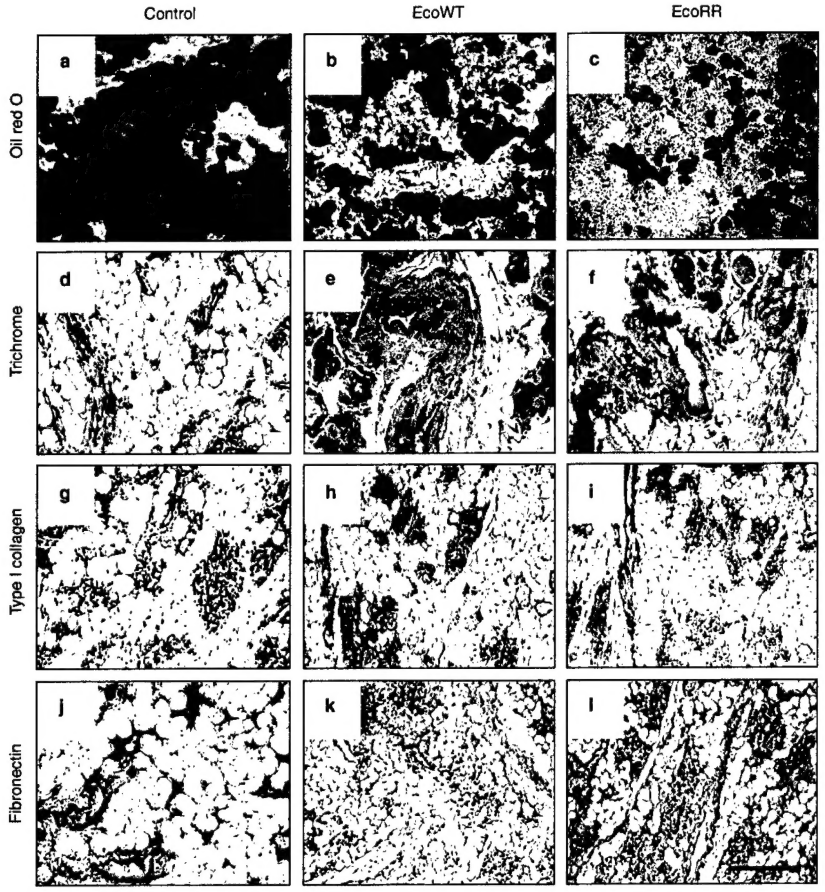

Figure 3 **Adipogenesis is reduced in female mice treated with ecotin during mammary-gland involution.** Animals were treated with carrier (control), WT ecotin (EcoWT) or EcoRR and examined after 5 days. **a–c**, Staining with Oil red O to detect adipocytes. **d–f**, Staining with Masson's Trichrome to detect collagen fibrils (blue). **g–i**, Immunohistochemistry to detect type I collagen (blue). **j–l**, Immunohistochemistry to detect fibronectin (blue). Scale bar represents 100 μm.

of physiological levels of exogenous human Plg restored adipose conversion to levels seen in normal human plasma (data not shown). These results show that Plg is required during adipocyte differentiation, when expression of ECM proteins, including fibronectin, is downregulated, and indicate that plasmin may be required to remodel the stromal ECM of preadipocytes.

Serine-protease inhibitors reduce adipogenesis during mammary-gland involution. We sought evidence that serine proteases function during adipogenesis *in vivo*. For this analysis we used the mammary gland, which has an adipose stroma. After lactation and weaning in the mouse, the mammary gland undergoes a programme of remodelling during involution to replace the secretory epithelial tissue involved in lactation with adipose tissue. Adipogenesis during involution occurs on a short timescale. Infiltration of adipocytes can be detected by day 2 of involution[14], and both uPA and tPA are upregulated during this process[15]. To evaluate serine-protease function *in vivo* during mammary adipogenesis, we treated female CF1 mice with WT ecotin or EcoRR over days 1–4 of involution, when the mammary gland is normally repopulated with adipocytes. On day 5, the density of adipose tissue of involution was greatly reduced in mammary glands treated with either form of ecotin (Fig. 3a–c). These data indicate that serine proteases have an important role in adipogenesis *in vivo*. Concomitant with the reduction in adipogenesis, deposition of stromal ECM, as shown by staining for collagen, increased significantly in mice treated with WT ecotin or EcoRR (Fig. 3e, f). We also observed increased deposition of the stromal proteins type I collagen (Fig. 3g–i) and fibronectin (Fig. 3j–l) in animals treated with either from of ecotin. WT ecotin, which does not inhibit uPA or plasmin, was as effective as EcoRR in blocking adipogenesis, and neither WT ecotin nor EcoRR inhibited tPA (Fig. 4). Surprisingly, when we examined epithelial apoptosis and involution[14], mice treated with EcoRR showed delayed epithelial involution, whereas those treated with WT ecotin did not (data not shown). These data indicate that neither uPA nor tPA is required for Plg activation during adipogenesis *in vivo*. Moreover, the lack of effect of WT ecotin on epithelial remodelling shows that differentiation of epithelia and adipocytes are not necessarily linked, but rather may be regulated independently.

Adipogenesis is impaired in Plg-deficient, but not uPA-deficient, mice. As Plg is required for 3T3-L1 adipogenesis, is it also critical *in vivo*? Plg-deficient mice[16] exhibited impaired adipogenesis (Fig. 4a, b) and increased collagen deposition in mammary glands (Fig. 4e, f), as was the case in mice treated with WT ecotin or EcoRR. This

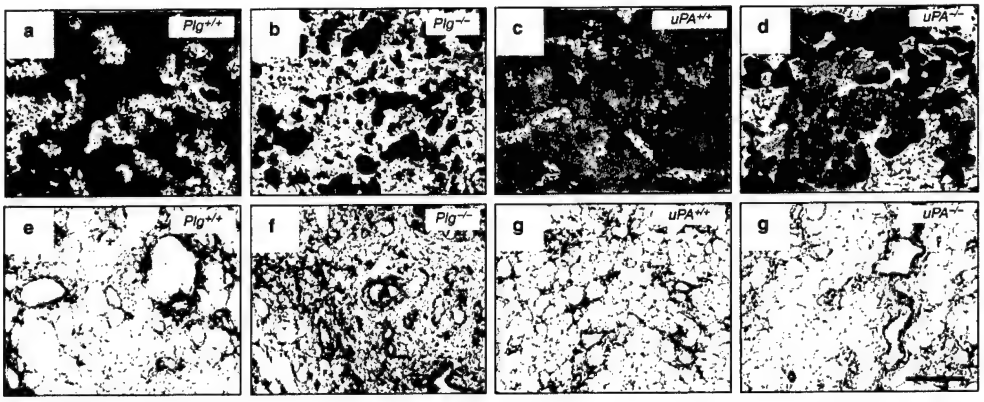

Figure 4 **Adipocyte differentiation is impaired during involution in Plg-deficient, but not uPA-deficient, mice. a–d**, Staining with Oil red O to detect adipocytes. **e–h**, Staining with Masson's Trichrome to detect collagen fibrils (blue). Scale bar represents 100 μm.

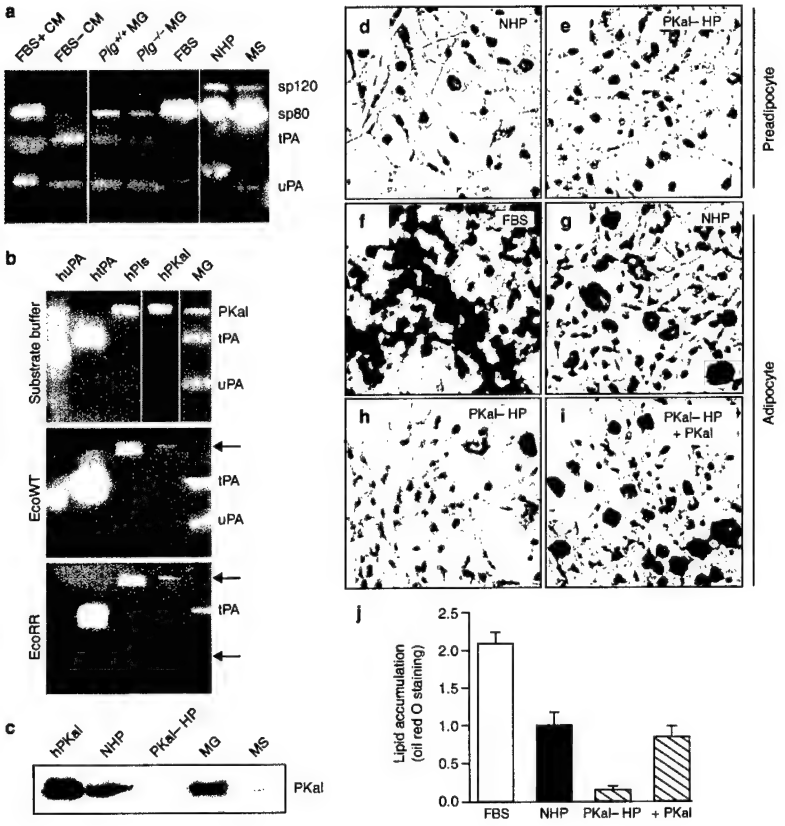

Figure 5 **PKal is present during adipogenesis and is required for differentiation of 3T3-L1 cells. a**, **b**, Casein/Plg zymograms. **a**, Incubation in substrate buffer. FBS, fetal bovine serum; CM, conditioned medium; MG, mammary-gland lysate; NHP, normal human plasma; MS, mouse serum. **b**, Incubation in substrate buffer alone or in buffer containing WT ecotin (EcoWT) or EcoRR. Inhibited bands are indicated by arrowheads.Human enzymes are given the prefix 'h'. Pls, plasmin. **c**, Western blotting to detect PKal. PKal− HS, prekallikrein-deficient human plasma. **d**, **e**, Staining with Oil red O of preadipocytes grown in normal (**d**) or prekallikrein-deficient (**e**) human plasma. **f–i**, Staining with Oil red O of adipocytes differentiated in FBS (**f**), normal human plasma (**g**), prekallikrein-deficient human plasma (**h**), or prekallikrein-deficient human plasma with exogenous human PKal added (**i**). **j**, Quantification of adipose conversion; absorbance is designated as 1.0 for cells grown in NHP. Data are means ± s.d.

indicates that Plg is required during involution for normal adipocyte differentiation. Interestingly, healthy adult *Plg*$^{-/-}$ mice of the same skeletal size, as confirmed using X-rays, were leaner and lighter than wild-type controls (at 23 weeks of age, *Plg*$^{-/-}$, 18.8 ± 2.1 g, $n = 4$; control, 22.8 ± 1.0 g, $n = 5$; $P < 0.005$). However, uPA did not seem to contribute significantly to adipocyte differentiation in the mammary gland. Mice lacking either uPA (Fig. 4c, d, g, h) or both uPA and tPA[17] (data not shown) showed no significant alteration in adipogenesis or collagen accumulation during involution. These data show that neither uPA nor tPA is required for adipogenesis in the mammary gland and therefore indicate the the possible presence of an alternative plasminogen activator during adipogenesis.

Plasma kallikrein is required during adipogenesis. We sought to identify another serine protease that is inhibited by both WT ecotin and EcoRR and can activate Plg. Lysates of involuting mammary gland at day 5 from either wild-type or *Plg*$^{-/-}$ mice, assayed by zymography on casein–Plg gels, showed the presence of a serine protease of M_r 80K, which was similar to the sp80 protease that was detected in medium conditioned by 3T3-L1 cells (Fig. 5a). sp80 was also present in normal mouse and human plasma, in FBS, and in the conditioned medium of 3T3-L1 cells grown in the presence, but not absence, of FBS. These data indicate that sp80 may be derived from plasma or serum, rather than from adipogenic cells.

Of the mammalian serine proteases that are present in databases, a compelling candidate is plasma kallikrein (PKal), which has a similar size and is inhibited by subnanomolar concentrations of WT ecotin[18]. Mouse sp80 and human PKal were inhibited both by WT ecotin and by EcoRR (Fig. 5b), whereas uPA was inhibited only by EcoRR. We identified sp80 as PKal by western blotting of mammary lysates and mouse serum with a polyclonal antibody against human prekallikrein (Fig. 5c). PKal has been shown to activate both pro-uPA[19,20] and Plg[21,22]. To investigate the function of PKal during adipocyte differentiation, we took advantage of Fletcher trait, a rare form of human plasma prekallikrein deficiency[23]. Both normal and prekallikrein-deficient human plasma supported growth of 3T3-L1 preadipocytes (Fig. 5d, e). Preadipocytes differentiated into adipocytes in normal human plasma, albeit to a lesser extent than in FBS (Fig. 5f, g). However, very little adipose conversion and only 14% lipid accumulation was observed in cells that were induced to undergo differentiation in prekallikrein-deficient human plasma (Fig. 5h, j). Addition of physiological levels of exogenous human PKal restored adipose conversion to 85% of that seen in normal human plasma (Fig. 5i, j). These data indicate that PKal is required for adipogenesis.

PKal and Plg promote adipogenesis under serum-free differentiation conditions. We sought to determine whether proteolysis by serine proteases promotes differentiation of 3T3-L1 cells. To this end, we induced the differentiation of 3T3-L1 preadipocytes in the absence of FBS. Under these conditions, cells underwent adipose conversion to a much lesser extent than cells differentiated in the presence of FBS (Fig. 6a, b, g). Addition of exogenous Plg did not enhance the extent of adipose conversion (Fig. 6c, g). However, addition of both Plg and PKal promoted adipose conversion to about 50% of that observed in FBS (Fig. 6a, d, g). PKal alone did not significantly increase adipose conversion (data not shown). The PKal zymogen, prekallikrein, was ineffective in promoting adipogenesis in both the presence and the absence of Plg (data not shown), indicating that activation of prekallikrein may also be required. Interestingly, Factor XII, the principal activator of prekallikrein, is also inhibited by nanomolar concentrations of ecotin[18]. The increase in adipose conversion observed in the presence of Plg and PKal was not significantly affected by addition of PAI-1 (Fig. 6e, g), but was reduced in the presence of EcoRR (Fig. 6f, g). These data indicate that although 3T3-L1 preadipocytes express both uPA and tPA (Fig. 2a), PKal is required during adipogenesis to activate Plg and promote adipose conversion.

A PKal-mediated Plg cascade promotes fibronectin cleavage during adipocyte differentiation. To evaluate our hypothesis that PKal activates Plg during adipocyte differentiation, we analysed the extent of Plg activation by 3T3-L1 cells by western blotting of the plasmin protease domain in the presence and absence of PKal. We first confirmed that PKal activates Plg at physiologically relevant concentrations, albeit to a lesser extent than that observed with uPA or tPA (Fig. 7a). However, PKal is present in plasma at relatively high concentrations (30–50 μg ml^{-1}; ref. 24) compared with uPA (3–5 ng ml^{-1}) or tPA (5–10 ng ml^{-1}; ref. 13). We next monitored activation of Plg during adipogenesis, and found that 3T3-L1 cells differentiated in the absence of FBS did not effectively activate Plg, and that addition of PKal significantly enhanced Plg activation (Fig. 7b). These data indicate that although 3T3-L1 cells express uPA and tPA (Fig. 2a), PKal may be required to activate Plg during 3T3-L1 differentiation.

We next sought to identify the molecular target of the Plg cascade.

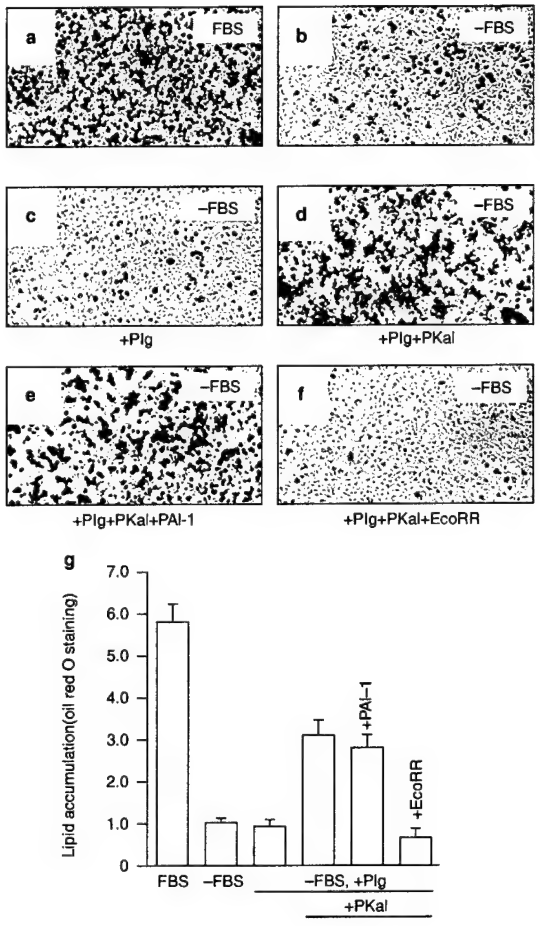

Figure 6 **Plg and PKal promote adipose conversion in the absence of FBS.** **a–f**, Staining with Oil red O of cells differentiated in the presence of FBS (**a**). in the absence of FBS (**b**). in the absence of FBS with the addition of exogenous Plg (**c**), in the absence of FBS with the addition of exogenous Plg and PKal (**d**), in the absence of FBS with the addition of exogenous Plg, PKal and PAI-1 (**e**), or in the absence of FBS with the addition of exogenous Plg, PKal and ecotin RR (**f**). **g**, Quantification of adipose conversion; absorbance is designated as 1.0 for cells grown in the absence of FBS (**b**) Data are means ± s.d.

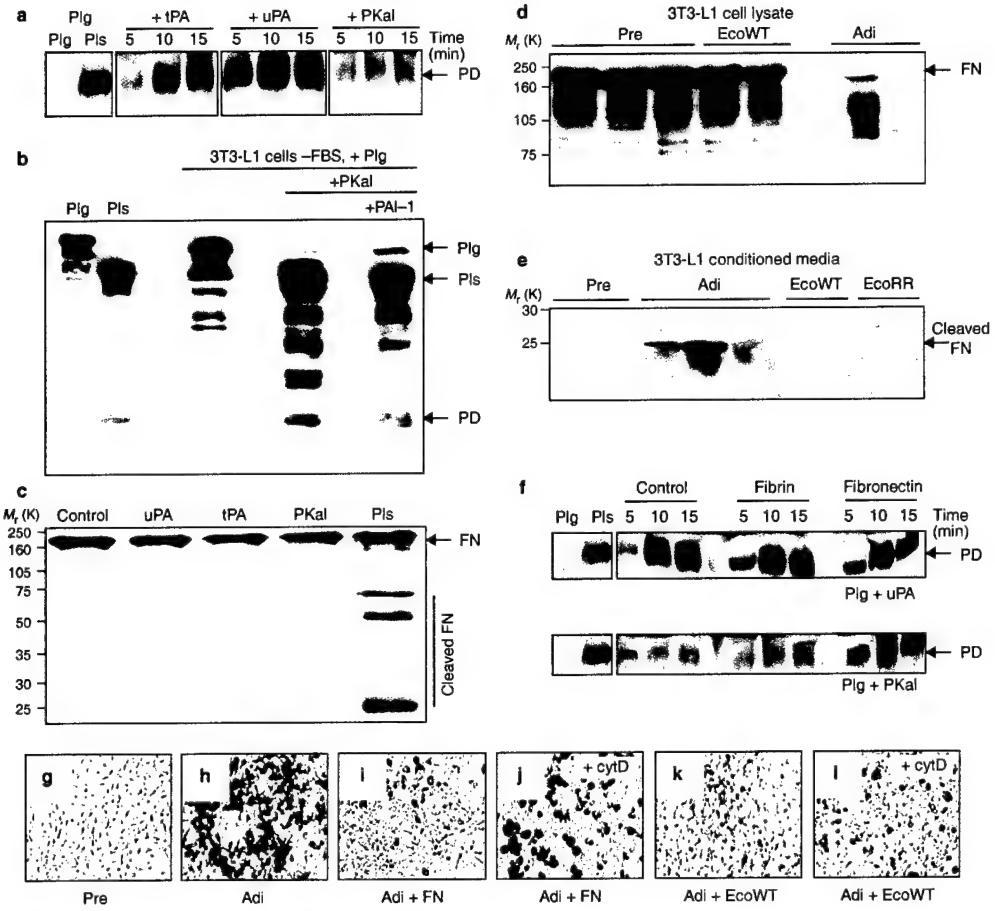

Figure 7 **PKal-mediated Plg activation promotes fibronectin degradation during adipocyte differentiation. a**, PKal activates Plg at physiologically relevant concentrations. Western blot showing generation of the M_r 25K protease domain (PD) of plasmin at 5, 10 and 15 min. **b**, Activation of Plg in the conditioned medium of 3T3-L1 cells is enhanced in the presence of PKal. Western blot of conditioned media from 3T3-L1 cells differentiated in the absence of FBS but with exogenous plasminogen (Plg), plasma kallikrein (PKal) or PAI-1, showing generation of plasmin (Pls) and the protease domain. **c**, Western blot (against human fibronectin) showing fibronectin (FN) cleavage products after incubation with serine proteases. **d**, Western blot (against rat fibronectin) of whole-cell lysates from preadipocytes (Pre), differentiated adipocytes (Adi) and cells differentiated in the presence of WT ecotin (EcoWT), showing that fibronectin is present in lysates from 3T3-L1 preadipocytes but is downregulated in adipocytes. **e**, Western blot (against endogenous mouse fibronectin) of conditioned media from preadipocytes, differentiated adipocytes, and cells differentiated in the presence of WT ecotin (EcoWT) and EcoRR, showing that fibronectin is cleaved during adipocyte differentiation. **f**, Western blot showing generation of the protease domain of plasmin at 5, 10 and 15 min in the absence (Control) and presence of fibrin and fibronectin. **g–l**, Staining with Oil red O of preadipocytes (**g**), of adipocytes (**h**) and of 3T3-L1 cells differentiated in the presence of fibronectin (**i**), fibronectin matrix and cytochalasin D (**j**), WT ecotin (**k**), or WT ecotin and cytochalasin D (**l**).

As increased deposition of fibronectin was observed in the mammary glands of ecotin-treated mice (Fig. 3j–l), we tested the hypothesis that the Plg cascade mediates fibronectin cleavage during adipocyte differentiation. We assayed uPA, tPA, plasmin and PKal for their ability to cleave fibronectin and found that only plasmin cleaves fibronectin into several fragments, including one of M_r 20K (Fig. 7c). Fibronectin was associated with 3T3-L1 preadipocytes and was downregulated in differentiated adipocytes, but not in cells treated with ecotin during differentiation (Fig. 7d) or in the absence of Plg (data not shown). When we analysed conditioned media for cleavage of endogenous mouse fibronectin during differentiation, we detected a cleaved fragment of M_r 20K in the conditioned medium of differentiated adipocytes, but not in that of preadipocytes or of cells cultured during differentiation with WT ecotin or EcoRR (Fig. 7e). Moreover, mammary lysates also generated fibronectin cleavage products that were suppressed by ecotin treatment (data not shown). These findings indicate that the Plg cascade may promote adipocyte differentiation by degrading the fibronectin-rich stromal ECM of preadipocytes.

PKal-mediated activation of the Plg cascade may be selective for plasmin generation in the region of the stromal ECM. We found that PKal-mediated, but not uPA-mediated activation of Plg is enhanced in the presence of fibronectin (Fig. 7f). tPA-mediated activation of Plg was enhanced by fibrin, but not by fibronectin (data not shown). These data indicate that PKal may be an important activator of Plg in fibrin-independent processes.

In support of a mechanism in which fibronectin degradation is

required during adipogenesis, we found that addition of an exogenous fibronectin matrix suppressed differentiation of 3T3-L1 cells (Fig. 7i). This suppression was overcome by addition of cytochalasin D, which disrupts the actin cytoskeleton and fibronectin at the cell surface (Fig. 7j). Similarly, the suppressive effects of ecotin were overcome by concomitant addition of cytochalasin D (Fig. 7k, l). These data indicate that remodelling of the stromal matrix of preadipocytes may be an important early step that promotes cell-shape change and expression of adipocyte-specific genes during differentiation.

Discussion

We have shown that extracellular proteolysis is a key mechanism for regulating adipocyte differentiation, and have demonstrated for the first time that PKal functions in the physiological Plg-activation cascade during adipogenesis. Although our *in vivo* study concentrated on the rapid and easily measurable adipogenesis in the mammary fat pad during mammary involution, our preliminary data clearly show the reduction of fat deposits at other sites, such as the epididymal fat pad in male $Plg^{-/-}$ mice (data not shown). However, because adipogenesis does eventually occur in the mammary gland and at other sites in $Plg^{-/-}$ mice, further proteolytic pathways may also contribute to adipocyte differentiation. We propose that the mammary fat pad during involution constitutes a rapid and sensitive system for evaluating the factors that regulate adipogenesis.

Surprisingly, uPA and tPA have relatively minor roles in adipogenesis both *in vivo* and in culture. uPA has been considered to be the primary enzyme involved in cell-mediated Plg activation by virtue of its high affinity for Plg and of the presence of a specific receptor, uPAR. However, mice lacking either the gene for uPA or the genes for both uPA and tPA do not have a marked phenotype with regard to adipogenesis, indicating the possible presence of other Plg activators. Other enzymes that have been implicated as Plg activators include PKal[21,22] and Factor XII[25]. PKal is a compelling candidate because of its high concentration, ubiquitous presence and ability to localize to the cell surface. It is also a potent activator of pro-uPA[26,27]. The requirement for PKal and Plg during adipogenesis indicates that PKal is a physiological component of the Plg-activation cascade. Although adipogenesis is attenuated in human plasma that lacks PKal or Plg, it remains to be determined whether this cascade has the same function in humans and mice as it does in culture. Our findings imply that PKal may have a significant role in other physiological and pathological processes that involve Plg activation *in vivo*.

It is clear from our results that proteolysis selectively affects terminally differentiating adipocytes rather than proliferating preadipocytes, as cleavage of cell-associated fibronectin, which is a substrate for plasmin, was regulated during adipocyte differentiation. How is the PKal–Plg system regulated during adipogenesis? During adipocyte differentiation, PKal may function as an activator of pro-uPA or as a direct activator of Plg. PKal-mediated activation of pro-uPA can occur on the surface of platelets[26] and of endothelial cells[27]. Although expression of uPA is regulated during 3T3-L1 differentiation, uPA-deficient mice do not exhibit an adipogenic phenotype, which leads us to favour the hypothesis that PKal directly activates Plg during adipogenesis. Our data indicate that PKal can activate Plg at physiologically relevant concentrations.

This raises the question of what the nature of the process that is regulated during adipogenesis. The functions of the PKal–Plg cascade may be regulated during differentiation by endogenous cell-surface receptors or inhibitors. One possibility is that binding to the cell surface is regulated. uPAR may serve as an acquired receptor for PKal. uPAR binds to pro-uPA at a site within uPAR domain 1 (ref. 28). The cleaved, two-chain form of high-molecular-mass kininogen, which is a substrate for PKal and contains a high-affinity binding site for prekallikrein[29], can also bind to uPAR through interactions within uPAR domains 2 and 3 (ref. 30). Thus, uPAR may function to promote PKal activity at the cell surface. However, uPAR is virtually undetectable in the involuting mammary gland[15], indicating that this is not the principal mechanism at this site. PKal activation is known to occur through Factor XII (ref. 20), which in turn requires activation by a cell-surface-dependent mechanism that may itself be regulated. Another model involves PAI-1, a serpin that inhibits both uPA and tPA[31], but not PKal (data not shown). Increased levels of PAI-1 are associated with obesity in mice and humans[32,33], and this protein is expressed by mature adipocytes in culture and *in vivo*[34]. PAI-1 may also function as a regulator of adhesion to the ECM[35]. However, the precise function of PAI-1 in development of adipose tissue is unclear. PAI-1 is barely detectable in the mammary gland during involution with its associated adipogenesis[15] and, moreover, our findings indicate that PKal, which is not inhibited by PAI-1, may function to promote adipocyte differentiation despite the presence of high PAI-1 levels observed in obesity.

How does extracellular proteolysis of the preadipocyte microenvironment facilitate adipogenesis? Our data support a model in which the Plg cascade is required for remodelling of the fibronectin-rich ECM of preadipocytes. This remodelling then gives rise to alterations in cell–ECM adhesion and cytoarchitecture, and promotes transcription of adipocyte-specific genes. Our finding that C/EBPβ and PPARγ, both of which are crucial to adipocyte differentiation, are only weakly induced in ecotin-treated cells, indicates that serine proteases may function at critical steps in adipocyte differentiation. Fibronectin is a component of the preadipocyte ECM — addition of exogenous fibronectin during differentiation of preadipocytes in culture inhibits cell-shape change and prevents adipogenesis — and is a substrate of plasmin[5] (Fig. 7). As differentiation of 3T3-L1 cells proceeds, synthesis of stromal ECM components such as fibronectin and fibrillar is reduced[36,37] and cleavage of fibronectin increases (Fig. 7). Thus, Plg activation results in rapid removal of fibronectin from the microenvironment of committed cells.

How does fibronectin function to suppress adipogenesis? One possibility is that cytoskeletal organization and signalling downstream of adhesion receptors for fibronectin foster a fibroblastic phenotype, whereas receptors for basement-membrane proteins foster an adipogenic phenotype. This hypothesis, which remains untested, is supported by the observation that cytochalasin D, which disrupts adhesion[38] and cytoskeletal structure, overcomes the suppressive effects of fibronectin and ecotin (Fig. 7j, l). A related, and also untested, hypothesis is that cleavage of fibronectin results in loss of syndecan, an integral membrane heparan sulphate proteoglycan that binds to fibronectin[39]. Loss of syndecan may downregulate Wnt signalling and thereby promote adipogenesis[40,41].

Alternatively, the Plg system may activate and release differentiation-promoting growth factors from sequestration in the stromal ECM. The bio-availability of IGF-I, a physiologically relevant regulator of adipocyte differentiation[42], is modulated by specific, high-affinity IGF-binding proteins (IGFBPs). Transgenic mice with increased IGFBP concentration exhibit impaired adipogenesis *in vivo*[43]. Plasmin and other serine proteases can cleave IGFBPs and release active IGF[44,45]. Thus, extracellular proteolysis is an important regulatory mechanism for the function of ECM molecules, as well as for cytokines, during adipogenesis. Whether the impact of proteolysis on fibronectin or IGFBPs is rate-limiting *in vivo* remains to be determined. Interestingly, matrix metalloproteinases also regulate adipogenesis both *in vivo* and in culture but, unlike the Plg system, their absence stimulates adipogenesis[46], indicating that the two classes of enzymes have distinct targets.

Plasmin acts in many fibrin-independent physiological and pathological processes, including neuronal cell death, cancer progression, and apoptosis of epithelial cells during mammary-gland involution. In the mammary gland, lack of Plg promotes survival of differentiated secretory epithelium[47], but inhibits adipocyte differentiation. Although there may be a reciprocal relationship between epithelial and mesenchymal cells to maintain tissue volume, it is also

clear from ecotin studies that these processes are regulated by activation of the Plg cascade by distinct components. The identities of the plasminogen activators that regulate other Plg-dependent processes remain to be determined. Our results have opened further avenues of research by which to elucidate the physiological functions of PKal, its activators, its target plasmin and their substrates. □

Methods

Preparation of ecotin.

Ecotins were prepared and purified as described[9]. Purified samples were tested and found to be free of endotoxin. Samples used for animal injections were diluted in PBS, pH 7.4.

Differentiation of 3T3-L1 cells.

3T3-L1 cells (American Type Culture Collection) were grown to confluence in DMEM containing 4.5 g l^{-1} glucose supplemented with 10% FBS (growth medium). Differentiation was induced by culturing cells in growth medium containing differentiation cocktail (0.22 μM insulin, 0.6 μM dexamethasone and 0.5 mM methylisobutylxanthine) as described[48]. Concurrently, 500 nM of WT ecotin, 500 nM EcoRR, 500 nM human PAI-1 (mutant human recombinant PAI-1; Calbiochem) or 2 μM human α2-AP (Calbiochem) was added to cells. Fresh growth medium was added to cells after 2 days; adipose conversion was analysed 6 days after induction.

To assess the effects of Plg depletion, FBS was passed over a lysine–Sepharose column several times and the flow-through fraction was collected[49]. Depletion of Plg from the flow-through fraction was confirmed by western blotting using a rabbit polyclonal antibody against human Plg (Dako, Carpinteria, California). 3T3-L1 cells were induced and maintained up to day 4 in medium containing 10% Plg-depleted FBS. For reconstitution experiments, 50 μg ml^{-1} human glu-type Plg (American Diagnostica Inc., Greenwich, Conneticut) was added to the medium. To assess the effects of Plg deficiency, 3T3-L1 cells were induced to differentiate without FBS in 5% pooled normal human plasma (George King Bio-Medical Inc., Overland Park, Kansas), Plg-deficient human plasma (American Diagnostica Inc.) or Plg-deficient human plasma reconstituted with 100 μg ml^{-1} human glu-type Plg for 2 days. Cells were maintained in fresh growth medium for a further 4 days.

To assess the effects of PKal deficiency, 3T3-L1 cells were induced to differentiate without FBS in 5% pooled normal human plasma, prekallikrein-deficient human plasma (George King Bio-Medical Inc.) or prekallikrein-deficient human plasma reconstituted with 50 μg ml^{-1} human PKal (Enzyme Research Laboratories, South Bend, Indiana) for 2 days. Cells were maintained in fresh growth medium for a further 4 days.

To assess the ability of serine proteases to promote differentiation under serum-free conditions, 3T3-L1 cells were induced to differentiate as described above but without FBS. Concurrently, 1 ∞M human glu-type Plg, 200 nM PKal, 500 nM PAI-1 and 500 nM EcoRR were added. Cells were maintained under these serum-free conditions until day 2 and were then switched to serum-containing growth medium for a further 4 days.

To assess the effects of fibronectin on 3T3-L1 differentiation, 6-well plates were coated with 50 μg ml^{-1} human fibronectin (Roche) at 4 °C for 12 h. Cells were grown and differentiated as described above. Cytochalasin D (0.5 μg ml^{-1}; Sigma) was added together with the differentiation cocktail. After 2 days cells were switched to growth medium.

In vivo adipocyte differentiation.

For ecotin treatment, female CF1 mice crossed with CD1 males were allowed to undergo normal pregnancy. The number of pups was normalized to 8 for each experiment and they were weaned after 7–10 days of lactation (day 0 of involution). Mice were injected intraperitoneally with 100 μg of WT ecotin, EcoRR or PBS twice a day on days 1–4 of involution and were killed on day 5 of involution. Each cohort contained four mice per treatment and experiments were repeated three times. Mammary glands from uPA-deficient C57BL/6 mice ($n = 6$), Plg-deficient C57BL/6 mice ($n = 7$), and wild-type littermate controls ($n = 6$ each) were collected on day 5 of involution. $Plg^{-/-}$ and wild-type littermates were weighed weekly at the ages of 4–25 weeks; weights were compared by ANOVA to calculate the P value. Mice lacking the genes for both uPA and tPA were generated as described[17]. To prepare frozen sections, tissue samples were snap-frozen in liquid nitrogen for biochemical analyses, placed in OCT and frozen; for paraffin sections they were fixed in 4% paraformaldehyde.

Oil red O staining, Masson Trichrome staining and immunohistochemistry.

3T3-L1 cells were stained with Oil red O as described[50]. Oil red O dye was extracted into isopropanol and absorbance was measured at 510 nm. Frozen sections of mammary gland (10 μm) were fixed in 50% ethanol and stained in a 0.2% Oil red O solution; they were then counterstained with Meyer's hematoxylin. Paraffin-embedded (CF1 mice) and frozen (uPA- and Plg-deficient mice and controls) tissue sections were stained using an Accustain™ Masson Trichrome Stain kit (Sigma). To detect fibronectin, paraffin sections were stained using a rabbit polyclonal antibody against rat fibronectin (Calbiochem). To detect type I collagen, paraffin sections were stained using a rabbit polyclonal type I antibody against mouse collagen (Calbiochem).

Substrate zymography and western blotting.

Frozen mammary tissue was homogenized in RIPA buffer (50 mM Tris–Cl pH 8.0, 150 mM NaCl, 1% NP40, 0.5% deoxycholate and 0.1% SDS) and the supernatant was collected. Conditioned media were collected from 3T3-L1 cells grown under normal and serum-free conditions. Cell lysates were prepared by scraping cells into RIPA buffer. 3T3-L1 nuclear lysates were prepared as described[51]. Mammary lysates were normalized to wet tissue weight; 3T3-L1 conditioned media and lysates were normalized to cell number. PPARγ was detected by western blotting of nuclear lysates using a goat polyclonal antibody raised against a peptide that maps within an internal region of human PPARγ (Santa Cruz). C/EBPβ was detected by western blotting of nuclear lysates using a rabbit polyclonal antibody raised against a peptide that maps at the carboxy terminus of rat C/EBPβ (Santa Cruz). For substrate zymography, samples were loaded onto non-reducing SDS–polyacrylamide gels containing 1 mg ml^{-1} casein and 10 μg ml^{-1} Plg[52]. Human tPA, high-molecular-mass uPA, plasmin (American Diagnostica Inc.) and PKal were used as controls. Gels were incubated overnight at 37 °C in the presence or absence of 500 nM WT ecotin or EcoRR. The identity of PKal was confirmed by western blotting using a sheep polyclonal antibody against human prekallikrein (Enzyme Research Laboratories).

Plasminogen activation and fibronectin cleavage.

To test PKal for its ability to activate Plg, 1 μM human glu-type Plg was incubated with 10 nM human high-molecular-mass uPA, 40 nM tPA or 40 nM PKal at 37 °C in activity buffer (50 mM Tris–Cl pH 7.5, 10 mM $CaCl_2$ and 0.01% Tween-20) on a 96-well plate coated with PBS (control), 50 μg ml^{-1} human fibronectin (Roche) or 2 mg ml^{-1} human fibrinogen (Sigma). Fibrinogen was converted to fibrin using 500 nM human thrombin (Sigma). Aliquots were removed after 5, 10 and 15 min and were reduced. Plg was detected by western blotting using a rabbit polyclonal antibody against human Plg (Dako). Reduced samples of human glu-type Plg and human plasmin were used as controls. To assay for Plg activation, 3T3-L1 cells were induced to differentiate under serum-free conditions as described above. At the time of induction, 1 μM human glu-type Plg, 200 nM PKal and 500 nM PAI-1 were added to the medium. Conditioned media were collected after 24 h and were reduced. Plg was detected by western blotting using the rabbit polyclonal antibody against human Plg.

To assay for fibronectin cleavage, 500 nM human plasma fibronectin was incubated with 10 nM human tPA, high-molecular-mass uPA, PKal or plasmin in activity buffer for 30 min at 37 °C. Cleavage products were reduced and subjected to 10% SDS–PAGE. Fibronectin was detected by western blotting using a monoclonal mouse antibody against human fibronectin (Calbiochem). To detect endogenous fibronectin, conditioned media and cell lysates were prepared from 3T3-L1 cells grown and differentiated in the presence of FBS. Cell-associated fibronectin was detected by western blotting of reduced 3T3-L1 cell lysates using a rabbit polyclonal antibody against rat fibronectin (Calbiochem). Cleaved mouse fibronectin present in conditioned media was reduced and assayed by western blotting using a rabbit antibody against mouse fibronectin (Gibco BRL).

RECEIVED 19 APRIL 2000; REVISED 28 SEPTEMBER 2000; ACCEPTED 15 NOVEMBER 2000; PUBLISHED 9 FEBRUARY 2001.

1. Hwang, C. S., Loftus, T. M., Mandrup, S. & Lane, M. D. Adipocyte differentiation and leptin expression. *Annu. Rev. Cell Dev. Biol.* **13**, 231–259 (1997).
2. Lowell, B. B. PPARγ: An essential regulator of adipogenesis and modulator of fat cell function. *Cell* **99**, 239–242 (1999).
3. Smas, C. M. & Sul, H. S. Control of adipocyte differentiation. *Biochem. J.* **309**, 697–710 (1995).
4. Cowherd, R. M., Lyle, R. E. & McGehee, R. E. Jr Molecular regulation of adipocyte differentiation. *Semin. Cell Dev. Biol.* **10**, 3–10 (1999).
5. Liotta, L. A. *et al.* Effect of plasminogen activator (urokinase), plasmin, and thrombin on glycoprotein and collagenous components of basement membrane. *Cancer Res.* **41**, 4629–4636 (1981).
6. Chen, Z. L. & Strickland, S. Neuronal death in the hippocampus is promoted by plasmin-catalyzed degradation of laminin. *Cell* **91**, 917–925 (1997).
7. Booth, B. A., Boes, M. & Bar, R. S. IGFBP-3 proteolysis by plasmin, thrombin, serum: heparin binding, IGF binding, and structure of fragments. *Am. J. Physiol.* **271**, E465–E470 (1996).
8. Chung, C. H., Ives, H. E., Almeda, S. & Goldberg, A. L. Purification from *Escherichia coli* of a periplasmic protein that is a potent inhibitor of pancreatic proteases. *J. Biol. Chem.* **258**, 11032–11038 (1983).
9. Wang, C. I., Yang, Q. & Craik, C. S. Isolation of a high affinity inhibitor of urokinase-type plasminogen activator by phage display of ecotin. *J. Biol. Chem.* **270**, 12250–12256 (1995).
10. Cao, Z., Umek, R. M. & McKnight, S. L. Regulated expression of three C/EBP isoforms during adipose conversion of 3T3-L1 cells. *Genes Dev.* **5**, 1538–1552 (1991).
11. Pairault, J. & Green, H. A study of the adipose conversion of suspended 3T3 cells by using glycerophosphate dehydrogenase as differentiation marker. *Proc. Natl Acad. Sci. USA* **76**, 5138–5142 (1979).
12. Kwaan, H. C. The plasminogen-plasmin system in malignancy. *Cancer Metastasis Rev.* **11**, 291–311 (1992).
13. Rijken, D. C. Plasminogen activators and plasminogen activator inhibitors: biochemical aspects. *Baillieres Clin. Haematol.* **8**, 291–312 (1995).
14. Lascelles, A. K. & Lee, C. S. in *Lactation: A Comprehensive Treatise* (ed. Larson, B. L.) 115–176 (Academic, New York, 1978).
15. Lund, L. R. *et al.* Two distinct phases of apoptosis in mammary gland involution: proteinase-independent and -dependent pathways. *Development* **122**, 181–193 (1996).
16. Bugge, T. H., Flick, M. J., Daugherty, C. C. & Degen, J. L. Plasminogen deficiency causes severe thrombosis but is compatible with development and reproduction. *Genes Dev.* **9**, 794–807 (1995).
17. Carmeliet, P. *et al.* Physiological consequences of loss of plasminogen activator gene function in mice. *Nature* **368**, 419–424 (1994).
18. Ulmer, J. S., Lindquist, R. N., Dennis, M. S. & Lazarus, R. A. Ecotin is a potent inhibitor of the contact system proteases factor XIIa and plasma kallikrein. *FEBS Lett.* **365**, 159–163 (1995).
19. Ichinose, A., Fujikawa, K. & Suyama, T. The activation of pro-urokinase by plasma kallikrein and its inactivation by thrombin. *J. Biol. Chem.* **261**, 3486–3489 (1986).
20. Hauert, J., Nicoloso, G., Schleuning, W. D., Bachmann, F. & Schapira, M. Plasminogen activators in dextran sulfate-activated euglobulin fractions: a molecular analysis of factor XII- and prekallikrein-dependent fibrinolysis. *Blood* **73**, 994–999 (1989).
21. Colman, R. W. Activation of plasminogen by human plasma kallikrein. *Biochem. Biophys. Res. Commun.* **35**, 273–279 (1969).
22. Miles, L. A., Greengard, J. S. & Griffin, J. H. A comparison of the abilities of plasma kallikrein, beta-Factor XIIa, Factor XIa and urokinase to activate plasminogen. *Thromb. Res.* **29**, 407–417 (1983).
23. Saito, H. *et al.* Heterogeneity of human prekallikrein deficiency (Fletcher trait): evidence that five of 18 cases are positive for cross-reacting material. *N. Engl. J. Med.* **305**, 910–914 (1981).
24. Raspi, G. Kallikrein and kallikrein-like proteinases: purification and determination by chromatographic and electrophoretic methods. *J. Chromatogr. B* **684**, 265–287 (1996).
25. Schousboe, I., Feddersen, K. & Rojkjaer, R. Factor XIIa is a kinetically favorable plasminogen activator. *Thromb. Haemost.* **82**, 1041–1046 (1999).

26. Loza, J. P., Gurewich, V., Johnstone, M. & Pannell, R. Platelet-bound prekallikrein promotes pro-urokinase-induced clot lysis: a mechanism for targeting the factor XII dependent intrinsic pathway of fibrinolysis. *Thromb. Haemost.* **71**, 347–352 (1994).
27. Lin, Y. *et al.* High molecular weight kininogen peptides inhibit the formation of kallikrein on endothelial cell surfaces and subsequent urokinase- dependent plasmin formation. *Blood* **90**, 690–697 (1997).
28. Behrendt, N. *et al.* The ligand-binding domain of the cell surface receptor for urokinase- type plasminogen activator. *J. Biol. Chem.* **266**, 7842–7847 (1991).
29. Tait, J. F. & Fujikawa, K. Identification of the binding site for plasma prekallikrein in human high molecular weight kininogen. A region from residues 185 to 224 of the kininogen light chain retains full binding activity. *J. Biol. Chem.* **261**, 15396–15401 (1986).
30. Colman, R. W. *et al.* Binding of high molecular weight kininogen to human endothelial cells is mediated via a site within domains 2 and 3 of the urokinase receptor. *J. Clin. Invest.* **100**, 1481–1487 (1997).
31. Dano, K. *et al.* Plasminogen activators, tissue degradation, and cancer. *Adv. Cancer. Res.* **44**, 139–266 (1985).
32. Samad, F. & Loskutoff, D. J. Tissue distribution and regulation of plasminogen activator inhibitor-1 in obese mice. *Mol. Med.* **2**, 568–582 (1996).
33. Juhan-Vague, I. & Alessi, M. C. PAI-1, obesity, insulin resistance and risk of cardiovascular events. *Thromb. Haemost.* **78**, 656–660 (1997).
34. Samad, F., Yamamoto, K. & Loskutoff, D. J. Distribution and regulation of plasminogen activator inhibitor-1 in murine adipose tissue *in vivo*. Induction by tumor necrosis factor-alpha and lipopolysaccharide. *J. Clin. Invest.* **97**, 37–46 (1996).
35. Loskutoff, D. J., Curriden, S. A., Hu, G. & Deng, G. Regulation of cell adhesion by PAI-1. *Apmis* **107**, 54–61 (1999).
36. Weiner, F. R., Shah, A., Smith, P. J., Rubin, C. S. & Zern, M. A. Regulation of collagen gene expression in 3T3-L1 cells. Effects of adipocyte differentiation and tumor necrosis factor alpha. *Biochemistry* **28**, 4094–4099 (1989).
37. Bortell, R., Owen, T. A., Ignotz, R., Stein, G. S. & Stein, J. L. TGF beta 1 prevents the down-regulation of type I procollagen, fibronectin, and TGF beta 1 gene expression associated with 3T3-L1 pre-adipocyte differentiation. *J. Cell Biochem.* **54**, 256–263 (1994).
38. Ali, I. U. & Hynes, R. O. Effects of cytochalasin B and colchicine on attachment of a major surface protein of fibroblasts. *Biochim. Biophys. Acta.* **471**, 16–24 (1977).
39. Tumova, S., Woods, A. & Couchman, J. R. Heparan sulfate chains from glypican and syndecans bind the Hep II domain of fibronectin similarly despite minor structural differences. *J. Biol. Chem.* **275**, 9410–9417 (2000).
40. Alexander, C. M. *et al.* Syndecan-1 is required for Wnt-1-induced mammary tumorigenesis in mice. *Nature Genet.* **25**, 329–332 (2000).
41. Ross, S. E. *et al.* Inhibition of adipogenesis by Wnt signaling. *Science* **289**, 950–953 (2000).
42. Smith, P. J., Wise, L. S., Berkowitz, R., Wan, C. & Rubin, C. S. Insulin-like growth factor-I is an essential regulator of the differentiation of 3T3-L1 adipocytes. *J. Biol. Chem.* **263**, 9402–9408 (1988).
43. Rajkumar, K., Modric, T. & Murphy, L. J. Impaired adipogenesis in insulin-like growth factor binding protein-1 transgenic mice. *J. Endocrinol.* **162**, 457–465 (1999).
44. Campbell, P. G. & Andress, D. L. Plasmin degradation of insulin-like growth factor-binding protein-5 (IGFBP-5): regulation by IGFBP-5-(201–218). *Am. J. Physiol.* **273**, E996–E1004 (1997).
45. Zheng, B., Clarke, J. B., Busby, W. H., Duan, C. & Clemmons, D. R. Insulin-like growth factor-binding protein-5 is cleaved by physiological concentrations of thrombin. *Endocrinology* **139**, 1708–1714 (1998).
46. Alexander, C. M., Selvarajan,S., Mudgett, J., & Werb, Z. Stromelysin-1 regulates adipogenesis during mammary gland involution. *J. Cell. Biol.* (in the press).
47. Lund, L. R. *et al.* Lactational development and involution of the mammary gland requires plasminogen. *Development* **127**, 4481–4492 (2000).
48. Bernlohr, D. A., Angus, C. W., Lane, M. D., Bolanowski, M. A. & Kelly, T. J. Jr Expression of specific mRNAs during adipose differentiation: identification of an mRNA encoding a homologue of myelin P2 protein. *Proc. Natl Acad. Sci.* USA **81**, 5468–5472 (1984).
49. Deutsch, D. G. & Mertz, E. T. Plasminogen: purification from human plasma by affinity chromatography. *Science* **170**, 1095–1096 (1970).
50. Ramirez-Zacarias, J. L., Castro-Munozledo, F. & Kuri-Harcuch, W. Quantitation of adipose conversion and triglycerides by staining intracytoplasmic lipids with Oil red O. *Histochemistry* **97**, 493–497 (1992).
51. Finbloom, D. S. *et al.* Growth hormone and erythropoietin differentially activate DNA-binding proteins by tyrosine phosphorylation. *Mol. Cell. Biol.* **14**, 2113–2118 (1994).
52. Talhouk, R. S., Chin, J. R., Unemori, E. N., Werb, Z. & Bissell, M. J. Proteinases of the mammary gland: developmental regulation in vivo and vectorial secretion in culture. *Development* **112**, 439–449 (1991).

ACKNOWLEDGMENTS

This work was supported by grants from the National Cancer Institute (to C.S.C. and Z.W.).

Correspondence and requests for materials should be addressed to Z.W.

THE JOURNAL OF BIOLOGICAL CHEMISTRY Vol. 275, No. 34, Issue of August 25, pp. 26333–26342, 2000

Cellular Localization of Membrane-type Serine Protease 1 and Identification of Protease-activated Receptor-2 and Single-chain Urokinase-type Plasminogen Activator as Substrates*

Received for publication, April 7, 2000, and in revised form, May 28, 2000
Published, JBC Papers in Press, May 30, 2000, DOI 10.1074/jbc.M002941200

Toshihiko Takeuchi‡§, Jennifer L. Harris‡, Wei Huang¶, Kelly W. Yan‖, Shaun R. Coughlin¶, and Charles S. Craik‡**

From the ‡Department of Pharmaceutical Chemistry and Biochemistry and Biophysics, ¶Cardiovascular Research Institute, University of California, San Francisco, California 94143 and ‖Center for Biomedical Laboratory Science, San Francisco State University, San Francisco, California 94132

Membrane-type serine protease 1 (MT-SP1) was recently cloned, and we now report its biochemical characterization. MT-SP1 is predicted to be a type II transmembrane protein with an extracellular protease domain. This localization was experimentally verified using immunofluorescent microscopy and a cell-surface biotinylation technique. The substrate specificity of MT-SP1 was determined using a positional scanning-synthetic combinatorial library and substrate phage techniques. The preferred cleavage sequences were found to be (P4-(Arg/Lys)P3-(*X*)P2-(Ser)P1-(Arg)P1′-(Ala)) and (P4-(*X*)P3-(Arg/Lys)P2-(Ser)P1(Arg) P1′(Ala)), where *X* is a non-basic amino acid. Protease-activated receptor 2 (PAR2) and single-chain urokinase-type plasminogen activator are proteins that are localized to the extracellular surface and contain the preferred MT-SP1 cleavage sequence. The ability of MT-SP1 to activate PARs was assessed by exposing PAR-expressing *Xenopus* oocytes to the soluble MT-SP1 protease domain. The latter triggered calcium signaling in PAR2-expressing oocytes at 10 nM but failed to trigger calcium signaling in oocytes expressing PAR1, PAR3, or PAR4 at 100 nM. Single-chain urokinase-type plasminogen activator was activated using catalytic amounts of MT-SP1 (1 nM), but plasminogen was not cleaved under similar conditions. The membrane localization of MT-SP1 and its affinity for these key extracellular substrates suggests a role of the proteolytic activity in regulatory events.

We recently reported the cloning and initial characterization of membrane-type serine protease 1 (MT-SP1)[1] from the PC-3 human prostatic cancer cell line (1). Northern blotting showed that MT-SP1 was strongly expressed in the gastrointestinal tract and the prostate, whereas lower expression levels were observed in the kidney, liver, lung, and spleen. The function of MT-SP1 and its possible role in pathological states are still undetermined. However, potent macromolecular inhibitors of MT-SP1 have been identified, and reagent quantities of a His-tagged fusion of the MT-SP1 protease domain were expressed in *Escherichia coli*, purified, and autoactivated (1). Biochemical characterization of the catalytic domain of MT-SP1 may provide insight regarding its physiological role.

MT-SP1 is predicted to be a modular, type II transmembrane protein that contains a signal/anchor domain, two complement factor 1R-urchin embryonic growth factor-bone morphogenetic protein domains, four low density lipoprotein receptor repeats, and a serine protease domain (1). The mouse homolog of MT-SP1, called epithin, recently was reported to be strongly expressed in fetal thymic stromal cells and highly expressed in a thymic epithelial nurse cell line (2). Another report describes the N-terminal sequencing of a protein called matriptase from human breast milk (3). The reported matriptase sequence is included in the translated sequence for the cDNA of MT-SP1. The matriptase cDNA reported appears to be a partial MT-SP1 cDNA, lacking 516 of the coding nucleotides. However, since the matriptase cDNA encodes a possible initiating methionine, alternative splicing could yield a protein lacking the N-terminal region of MT-SP1.

Although MT-SP1 and epithin are predicted to be type II transmembrane proteins, the reported matriptase cDNA lacks the 5′ end of the MT-SP1 cDNA and therefore the translated sequence lacks the signal/anchor domain, leading to a predicted secreted protein. Determining the cellular localization of the protein could help resolve this discrepancy and may also provide clues for understanding the function of the protein. For example, another structurally similar membrane-type serine protease, enteropeptidase, is involved in a proteolytic cascade by which activation of trypsinogen leads to activation of other digestive proteases (4). The membrane localization is essential to restrict the activation of trypsinogen to the enterocytes of the proximal small intestine. Since MT-SP1 is also predicted to be a membrane-type protease, localization to the membrane may be essential to the proper function of the enzyme. The localization of MT-SP1 is addressed in this work using immunofluorescent localization, immunoblot analysis, and cell-surface biotinylation experiments.

Further understanding of the role of MT-SP1 may be obtained by characterizing the activity of the protease domain. Reagent quantities of a His-tagged fusion of the MT-SP1 protease domain were expressed in *E. coli*, purified, and autoactivated, allowing determination of MT-SP1 substrate specificity.

* This work was supported in part by National Instututes of Health Grant CA72006, Developmental Research Program of the University of California, San Francisco, Prostate Cancer Center, and by the Daiichi Research Center. The costs of publication of this article were defrayed in part by the payment of page charges. This article must therefore be hereby marked "*advertisement*" in accordance with 18 U.S.C. Section 1734 solely to indicate this fact.

§ Supported by National Instututes of Health Postdoctoral Fellowship CA71097 and Department of Defense Prostate Cancer Research Program Postdoctoral Fellowship DAMD17-99-1-9515.

** To whom correspondence should be addressed. Tel.: 415-476-8146; Fax: 415-502-8298; E-mail: craik@cgl.ucsf.edu.

[1] The abbreviations used are: MT-SP1, membrane-type serine protease 1; sc-uPA, single-chain urokinase-type plasminogen activator; PAR, protease-activated receptor; PS-SCL, positional scanning-synthetic combinatorial library; PBS, phosphate-buffered saline; PNGase, peptide *N*-glycosidase; AMC, 7-amino-4-methylcoumarin.

Synthetic substrates are typically used to determine the specificity of proteases. However, the use of single substrates can be tedious for synthetic peptide substrates that contain multiple amino acid residues; the exhaustive analysis of each substrate for all combinations of amino acids at multiple positions rapidly becomes impractical. By using pools of substrates through combinatorial techniques, rapid determination of the full specificity profile for an enzyme can be obtained. Two methods have been employed to determine the substrate specificity of the MT-SP1 protease domain as follows: positional scanning synthetic combinatorial libraries (PS-SCL) (5–8) and substrate phage display (8–10).

PS-SCL of fluorogenic peptide substrates has been a very powerful tool for determining protease specificity for proteases that require an Asp in the P1[2] (11) position (6–8). However, the synthetic strategy used to make the P1-Asp library is not generalizable to all amino acids. However, a strategy allowing diversity at P1 has been achieved through nucleophilic displacement of the peptide library from the solid support by condensation with a fluorogenic 7-amino-4-methylcoumarin (AMC)-derivatized amino acid (12). This strategy was used to create a PS-SCL library with the general structure Ac-*X*-*X*-*X*-Lys-AMC (12), and can be applied to enzymes such as MT-SP1 that have basic P1 specificity. Since PS-SCL cannot be used to determine the specificity C-terminal to the scissile bond (prime side, P1′,P2′, . . . ,P*n*′) due to the requirement of the AMC in the P1′ position, substrate phage display was utilized (8–10). An inexpensive, accessible phage display technique utilizes a cleavable peptide sequence that is inserted between a histidine tag affinity anchor and the M13 phage coat protein, pIII. Bacteriophage containing preferred peptide recognition sequences for a given protease are cleaved from the resin, recovered, and amplified, whereas uncleaved phage remain bound to the Ni(II) resin. After several rounds of cleavage and subsequent amplification of the phage, the phagemid DNA plasmids can be sequenced and analyzed for protease substrate specificity preferences (8).

Together, these techniques allowed the determination of the extended substrate specificity of MT-SP1; this specificity was used to identify protease-activated receptor 2 (PAR2) and single-chain urokinase-type plasminogen activator (sc-uPA) as macromolecular substrates of MT-SP1. PAR2 is expressed in vascular endothelial cells and in a variety of epithelial cells and may function in inflammation, cytoprotection, and/or cell adhesion (13–16), whereas uPA has been implicated in tumor cell invasion and metastasis (17, 18). Therefore, this study raises potential biological and pathological consequences of MT-SP1 activity.

EXPERIMENTAL PROCEDURES

Materials—All primers used were synthesized on an Applied Biosystems 391 DNA synthesizer. All restriction enzymes were purchased from New England Biolabs (Beverly, MA). Automated DNA sequencing was carried out on an Applied Biosystems 377 Prism sequencer, and manual, chain termination, DNA sequencing was carried out under standard conditions. Deglycosylation was performed using PNGase F (New England Biolabs, Beverly, MA). All other reagents were of the highest quality available and purchased from Sigma or Fisher unless otherwise noted.

Antibody Production and Immunoblot Analysis—Polyclonal antiserum against purified His-MT-SP1 protease domain was raised in rabbits (Covance Corp., Richmond, CA). This antiserum was further purified by binding and elution from an antigen column, which had the His tag fusion of the inactive Ser-805→ Ala MT-SP1 protease domain covalently linked to the column using *N*-hydroxysuccinimide-activated Sepharose 4 Fast Flow (Amersham Pharmacia Biotech). Immunoblot analysis was performed as described previously (19). Antibody-bound protein bands were detected using a goat anti-rabbit horseradish peroxidase-conjugated secondary antibody (Pierce) and enhanced chemiluminescence (Amersham Pharmacia Biotech).

Cell Culture and Immunofluorescence—The PC-3 (CRL-1435) and HeLa S3 (CCL-2.2) cell lines were purchased from ATCC (Manassas, VA) and grown according to the instructions provided by ATCC. The

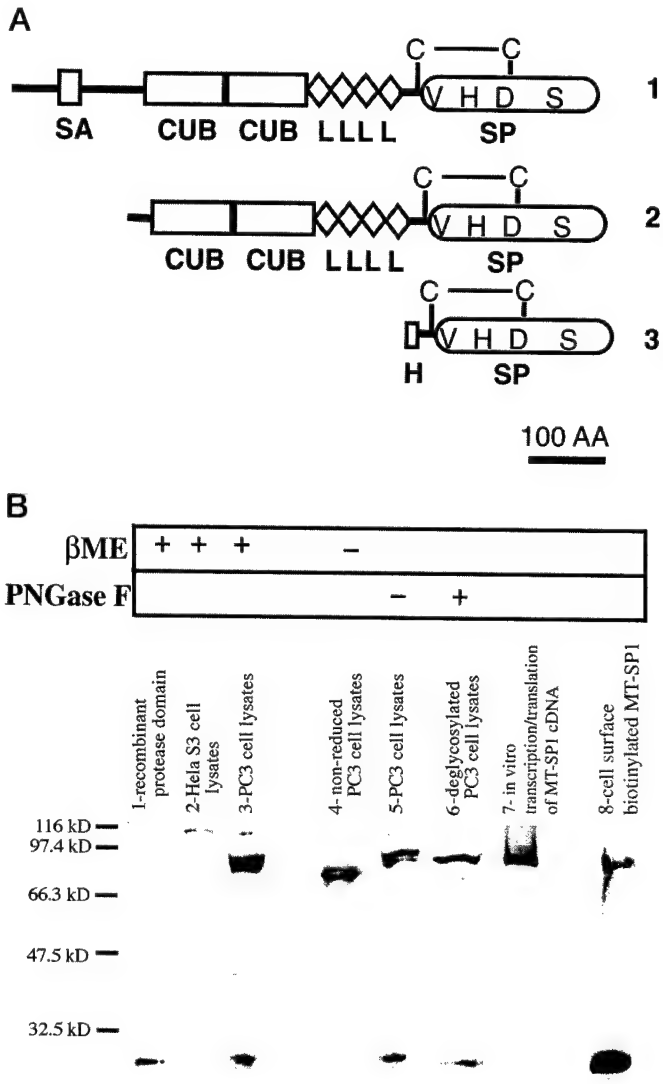

FIG. 1. *A*, the proposed domain structure of human MT-SP1. *SA* represents a possible signal anchor, *CUB* represents a repeat first identified in complement components C1r and C1s, the urchin embryonic growth factor and bone morphogenetic protein 1 (51), *L* represents low density lipoprotein receptor repeat (52), *SP* represents a chymotrypsin family serine protease domain (45). The predicted disulfide linkages are shown labeled as *C–C*. *2*, the proposed translation of matriptase. *3*, recombinant, soluble MT-SP1 serine protease domain, where *H* represents a 6-histidine tag. *B*, immunoblot analysis of recombinant MT-SP1 protease domain and analysis of PC-3 and HeLa cell lysates, *in vitro* transcription/translation of MT-SP1 cDNA, and identification of cell-surface biotinylated MT-SP1. Recombinant MT-SP1 is shown in *1st lane*. MT-SP1 is not expressed by HeLa S3 cells, *2nd lane*. Full-length native MT-SP1 appears at 87 kDa and the native protease domain at 30 kDa, *3rd lane*. The protease domain does not appear in immunoblots when the PC3 cell lysates are run under non-reducing conditions ((−)-β-mercaptoethanol (*βME*)), corroborating the predicted disulfide linkage between the MT-SP1 pro-domain at Cys-604 and the catalytic protease domain at Cys-731 (*4th lane*). Deglycosylation of the PC-3 cell lysates is shown in the *6th lane* (+ *PNGase F*) compared with similarly treated nondeglycosylated PC3 cell lysates, *5th lane*. *In vitro* transcription/translation of full-length MT-SP1 cDNA, *7th lane*. Immunoblotting of cell-surface biotinylated MT-SP1, *8th lane*.

[2] The nomenclature for the substrate amino acid preference is Pn, Pn-1, . . . P2, P1, P1′, P2′, . . . ,Pm-1′,Pm′. Amide bond hydrolysis occurs between P1 and P1′. Sn, Sn-1, . . . , S2, S1′, S2′, . . . , Sm-1′, Sm′ denotes the corresponding enzyme-binding sites (11).

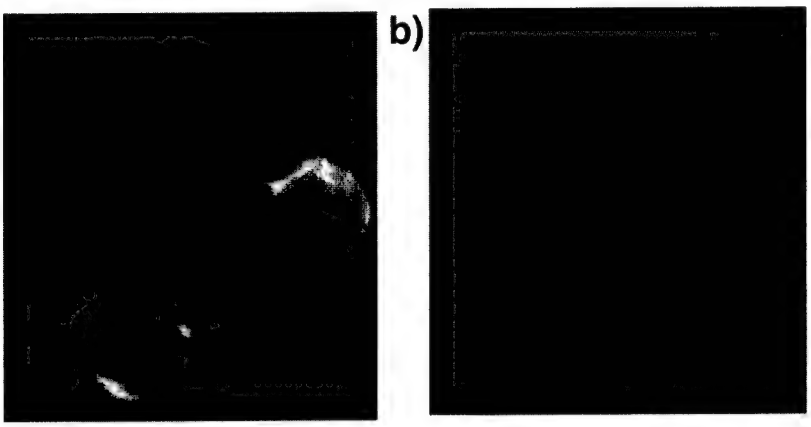

FIG. 2. **Immunofluorescence reveals extracellular surface localization of MT-SP1.** PC-3 cells treated with MT-SP1 antiserum are shown in *a*. HeLa S3 cells treated with MT-SP1 antiserum are shown in *b*, negative control.

cells were plated on glass coverslips and were stained as described previously (20). Permeabilization was performed with 0.5% Triton X-100 in phosphate-buffered saline (PBS). Non-permeabilized cells were treated with PBS. The primary antibody was either affinity-purified anti-MTSP1 at 1:500 dilution, monoclonal anti-uPAR antibody at 1:500 dilution, or an anti-vimentin antibody at 1:100 dilution in 5% goat serum. The appropriate biotinylated anti-mouse or anti-rabbit secondary antibody (Jackson ImmunoResearch, West Grove, PA) was used at 1:1000 dilution in 5% goat serum. Subsequently, the cells were treated with fluorescein isothiocyanate-conjugated streptavidin at 1:500 dilution in 5% goat serum. Coverslips were mounted using Gel Mount (Biomeda, Foster City, CA), and samples were imaged using an Olympus BX60 fluorescent microscope. Each of the antibody incubation steps were for an hour with three 5-min PBS washes in between each antibody incubation. Cell lysates were prepared using PBS containing 1% Triton X-100 and 5 mM EDTA.

Cell-surface Biotinylation—The cell-impermeable sulfosuccinimidobiotin (Pierce) was used to biotinylate surface proteins as described earlier (21). Greater than 95% of the cells remained impermeable as assayed by the impermeability of the cells to trypan blue. Cell lysates were prepared using PBS containing 1% Triton X-100 and 5 mM EDTA. Biotinylated proteins were captured using streptavidin-agarose (Life Technologies, Inc.) and electrophoresed on a 10% SDS-polyacrylamide gel. Immunoblot analysis was performed as described above. No MT-SP1 was observed in the non-biotinylated PC-3 extracts.

Creation of a P1-Lysine Positional Scanning Combinatorial Library—The detailed synthesis and characterization of the combinatorial library used in this study are described elsewhere (12). Three support-bound sub-libraries were prepared (P2, P3, and P4) employing an alkane sulfonamide linker (22) and solid-phase peptide synthesis. Each sub-library consisted of 19 resins (one unnatural amino acid, norleucine, was included, but cysteine and methionine were excluded) for which a single position was spatially addressed by the coupling of a single amino acid. The two remaining positions of each resin were supplied by the coupling of isokinetic mixtures of amino acid derivatives (23) to give a resin-bound mixture of 361 different peptides. The 57 resins comprising the entire PS-SCL were put into individual wells and cleaved from the resin with a lysine-coumarin derivative. Filtration, side chain deprotection, and concentration provided a PS-SCL of 57 wells containing 361 tetrapeptide-coumarin derivatives per well for a total of 6,859 peptide substrates per library.

Enzymatic Assay of the PS-SCL—The concentration of MT-SP1 was determined by active-site titration as described earlier (1). Substrates from the PS-SCL were dissolved in Me_2SO. Approximately 2.5×10^{-9} mol of each sub-library (361 compounds) were added to 57 wells of a 96-well Microfluor White "U" bottom plate (Dynex Technologies, Chantilly, VA). Final substrate concentration was approximately 0.25 μM, making the hydrolysis of the AMC group directly proportional to the specificity constant, k_{cat}/K_m. Hydrolysis reactions were initiated by the addition of enzyme (1 nM) and monitored fluorometrically with a Perkin-Elmer LS50B Luminescence Spectrometer 96-well plate reader, with excitation at 380 nm and emission at 460 nm. Assays were performed in a buffer containing 50 mM Tris, pH 8.8, 100 mM NaCl, 1% Me_2SO (from substrates), and 0.01% Tween 20.

Creation of His-tagged Substrate Phage Libraries—The phagemid pHisX3P3, derived from pBS, was used as described previously (8). In the biased library, the cleavage sequence was based upon the consensus sequence derived from the PS-SCL library results (*X*-(Arg/Gln/Lys)-(Ser/Ala/Gly)-Arg-*XX*), where *X* can encode any amino acid in the P4 position; P3 encodes at least arginine, glutamine, and lysine; P2 encodes at least serine, alanine, and glycine; P1 is fixed as arginine; and both P1′ and P2′ are completely randomized. In the unbiased library, the randomized peptide sequence encoded in the vector is *XXXRX*, where *X* can encode any amino acid. In this cleavage sequence, P1 is fixed as arginine, and P4–P2 and P1′ are randomized. The degenerate oligonucleotides synthesized to create the library contained the following randomized sequences (where N indicates equimolar concentrations of A, C, G, and T; S indicates equimolar concentrations of G and C; M indicates equimolar mixtures of A and C; R indicates equimolar mixtures of A and G; and K indicates equimolar mixtures of G and T): NNS MRG KSS AGG NNS NNS (biased library) and NNS NNS NNS AGA (unbiased library). The phage library and phagemid vector were constructed by ligation into the cut pHisX3P3 vector followed by electroporation of the ligated vector into XL2-Blue MRF′ cells (Stratagene, La Jolla, CA) as described earlier (8). In the biased library, the transformation efficiency was 2.4×10^7 individual clones, and the transformation efficiency of the unbiased library was 2.1×10^7 individual clones, allowing for >99% completeness of each library.

His-tagged Substrate Phage Cleavage—Two hundred microliters of nickel(II)-nitrilotriacetic acid resin (Qiagen, Santa Clarita, CA) was washed with 10 ml of activity buffer (50 mM Tris, pH 8.8, 100 mM NaCl, 0.1% Tween 20). Phage particles (10^9) were added to the washed Ni(II) resin and bound with gentle agitation for 1 h. The Ni(II) resin subsequently was washed with 5 ml of activity buffer and gently agitated for 30 min. This washing step was repeated for a total of four 30-min washes. The activity buffer was removed, and the bound phage were eluted twice with 0.5 ml of activity buffer containing 0.5 M imidazole. The imidazole was removed using a PD-10 column (Amersham Pharmacia Biotech). The resulting solution was concentrated to a volume of 0.5 ml using a Centricon-100 filter concentrator (Millipore, Bedford, MA). The phage then were cleaved with 1 nM recombinant MT-SP1 protease domain for 1 h at 37 °C. A control sample lacking MT-SP1 was used to monitor binding of uncleaved phage to the Ni(II) resin. The cleaved phage were added to 200 μl of washed Ni(II) resin to rebind uncut phage and allowed to bind for 3 h. Phage that are cleaved by MT-SP1 lack the His tag and will not bind to Ni(II) resin. These unbound phage were eluted and amplified as described earlier (8), and the cleavage round was repeated. Five rounds of panning were completed with the biased library before sequencing, and eight rounds of panning were performed for the unbiased library.

Molecular Modeling of the MT-SP1·Substrate Complex—All modeling was performed using the Biopolymer and Homology modules within Insight II (Molecular Simulations, San Diego). The MT-SP1 amino acids were threaded onto the β-tryptase crystal structure (24) (Protein Database code 1AOL). A model of an inhibitor bound MT-SP1 structure was produced by using a trypsin-ecotin crystal structure (25). The trypsin-ecotin crystal structure was modeled onto the MT-SP1 structure by overlaying the trypsin and MT-SP1 protease domains; subsequently the trypsin was removed from the model. The active-site protease binding loop of ecotin was used as a model of a substrate binding to the MT-SP1 active site. The preferred side chain rotamers of the modeled substrate were explored manually to maximize interaction with the MT-SP1 active site.

Assay for PAR Activation—cDNAs encoding hPAR1, mPAR2, hPAR3, and hPAR4 tagged with a FLAG epitope were used (26–29). *Xenopus* oocytes were microinjected with 25 ng of hPAR1, 0.25 ng of mPAR2, 25

ng of hPAR3, and 2 ng of hPAR4 cRNA per oocyte. ^{45}Ca release triggered by soluble MT-SP1 protease domain was measured (26). PAR expression on the oocyte surface was quantitated using a colorometric assay that measures the level of the FLAG tag, which was displayed at the extracellular N terminus of each PAR (26, 30).

Cleavage of sc-uPA—sc-uPA (5 μM) was incubated with MT-SP1 (1 nM) in 50 mM Tris, pH 8.8, 100 mM NaCl at 37 °C. At specified intervals, an aliquot was withdrawn and split into two portions. The first portion was assayed for activity against Spectrozyme UK (carbobenzoxy-L-γ-glutamyl(α-*t*-butoxy)-glycyl-arginine-*p*-nitroanilide; American Diagnostica, Greenwich, CT), and the second portion was boiled in sample buffer (125 mM Tris-HCl, pH 6.8, 4% SDS, 10% 2-mercaptoethanol, 20% glycerol) and subjected to immunoblot analysis. Immunoblots were prepared as described above for anti-MT-SP1 immunoblots, except that polyclonal rabbit anti-human uPA antibodies (American Diagnostica, Greenwich, CT) were used as the primary antibody.

RESULTS

Migration Pattern in SDS-PAGE and Cell-surface Localization of MT-SP1—MT-SP1 is predicted to be a 95-kDa protein, and upon activation of the protease domain, a disulfide link is predicted to tether the catalytic domain to the non-catalytic domains (Fig. 1*A*). Under non-reducing conditions, immunoblotting of Triton extracts derived from PC-3 cells shows a doublet at approximately 80 kDa (Fig. 1*B, 4th lane*) using polyclonal antibodies directed against the soluble, recombinant MT-SP1 protease domain (Fig. 1, *A* and *B, 1st lane*). Under reducing conditions, the predicted disulfide linkage between the catalytic and non-catalytic domain should be severed, resulting in release of the proteolytic domain. Indeed a band at 87 kDa and a band at 29 kDa are observed (Fig. 1*B, 3rd* and *5th lanes*). Upon deglycosylation of the PC-3 Triton extract with PNGase F, only a single band is observed at 85 kDa, and the band attributed to the protease domain decreases to the size of the recombinant MT-SP1 (Fig. 1*B, 6th lane*). This proposed glycosylation is consistent with the predicted *N*-linked glycosylation sites in the pro-domain (residues 109, 302, and 485) and the protease domain (residue 771) (see Ref. 1). The band at 85 kDa is smaller than the predicted 95 kDa of the full-length protein. This decrease in size may be due to significant folding of the protease even under reducing conditions with SDS. This decrease in size appears more pronounced under non-reducing conditions in the presence of SDS (Fig. 1*B, 4th lane*), where the protease domain appears to be only 80 kDa in size. *In vitro* transcription-translation of full-length MT-SP1 cDNA results in a band at 85 kDa (Fig. 1*B, 7th lane*), which is the same size as the deglycosylated MT-SP1 (Fig. 1*B, 6th lane*), supporting the hypothesis that the full-length protein runs smaller than the predicted molecular weight. The absence of the band at 29 kDa in this sample is presumably due to the reducing environment in the *in vitro* transcription/translation mixture, which likely prevents proper folding and activation of the protease.

MT-SP1 is predicted to be an integral membrane protein localized to the extracellular surface through a signal/anchor domain (1). The extracellular surface localization of MT-SP1 was verified using two independent techniques, biotinylation of cell-surface proteins and immunofluorescence. Cell-surface localization was determined by biotinylating cell-surface proteins using a non-permeable biotinylation reagent (21, 31). After removal of unreacted biotin, the cells are lysed with 1% Triton X-100 and 5 mM EDTA in PBS, and biotinylated proteins are bound to streptavidin-immobilized agarose. SDS-PAGE followed by immunoblotting with anti-MT-SP1 antibodies showed the presence of MT-SP1 in the biotinylated cell lysate (Fig. 1*b, 8th lane*), whereas no MT-SP1 was observed in the non-biotinylated lysate (data not shown). The non-permeability of the cells was verified with trypan blue, which showed that >95% of the cells were intact. The extracellular localization of MT-SP1 was independently verified using immunofluorescent microscopy. Fig. 2*A* shows extracellular staining of PC-3 cells under non-permeabilizing conditions when treated with rabbit antiserum directed against the MT-SP1 protease domain. Similar staining patterns are observed with treatment against the urokinase plasminogen activator receptor (data not shown). The specificity of anti-MT-SP1 antigen interaction was characterized using both recombinant MT-SP1 (Fig. 1*B, 1st lane*) and HeLa S3 cells, which do not express MT-SP1 (Fig. 1*B, 3rd lane*). Little fluorescence staining is observed for HeLa S3 cells (Fig. 2*B*), suggesting that the observed immunostaining in PC-3 cells is due to specific interaction of the antibodies with MT-SP1 protein. It should be noted that expression in COS cells of MT-SP1, in which the signal/anchor domain was deleted, resulted in MT-SP1 that remained bound to the cell surface (data not shown), suggesting that domains other than the signal/anchor are involved in cell-surface interactions.

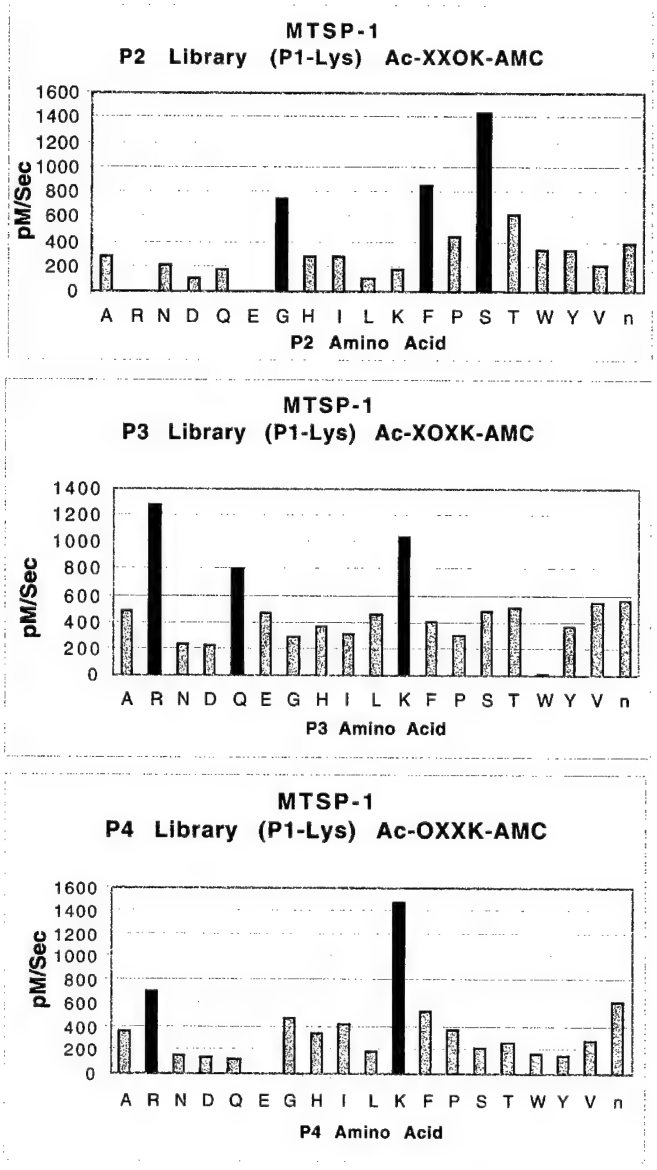

FIG. 3. **Activity of MT-SP1 in a P1-Lys positional scanning-synthetic combinatorial library.** *Y* axis is pM of fluorophore released per s. *x* axis indicates the amino acid held constant at each position, designated by the one-letter code (*n* represents norleucine).

Determination of MT-SP1 Substrate Specificity—When a PS-SCL library with the general structure Ac-*X*-*X*-*X*-Lys-AMC (12) was used to profile MT-SP1, the specificity was found to be (P4 = Lys → Arg; P3 = Arg/Lys/Gln; P2 = Ser → Phe/Gly) (Fig.

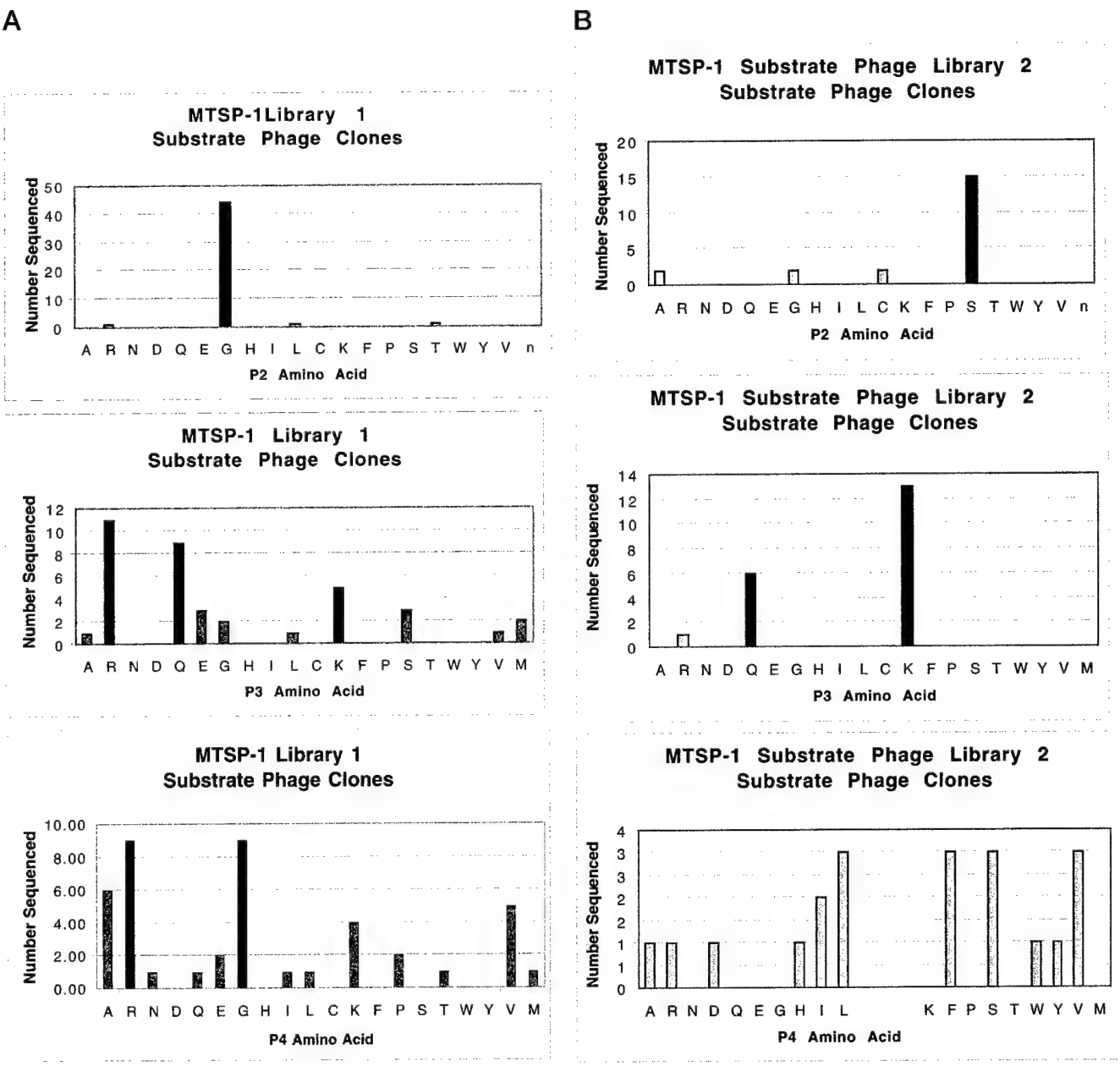

FIG. 4. **Cleavage frequency of amino acids in substrate phage clones.** *A*, P4–P2 cleavage frequency is shown for the unbiased substrate phage library from rounds 5 and 8. *B*, P4–P2 cleavage frequency is shown for the biased substrate phage library from round 5.

3). Thus the basic residues lysine and arginine are preferred residues at the P4 position, whereas these basic residues as well as glutamine are preferred at the P3 position. Interestingly, glycine, serine, and phenylalanine are all well tolerated at P2, despite their difference in size and hydrophobicity. The preference for phenylalanine at the P2 position is not a result of a biased library, since this library has been used to profile other enzymes such as thrombin, and phenylalanine was not cleaved efficiently at this position (12). This affinity for phenylalanine in the P2 position was also validated using macromolecular substrates, described below.

Two substrate phage libraries were utilized to determine the substrate specificity C-terminal to the scissile bond and to determine whether there are any interdependences among the enzyme subsites. The first phage display library was an unbiased library in which P1 was fixed as Arg, whereas P4–P2 and P1′ were completely randomized. The results of this library are shown in tabular form in Table I, where individual peptide cleavage sequences can be observed. However, the overall cleavage affinities for a given subsite are better displayed in graphical format as shown in Fig. 4*A*. The substrate specificity observed in substrate phage display match closely with the results from the PS-SCL (Fig. 3). In this phage display library, basic residues appear in P4, although it is not to the same extent observed in the PS-SCL. Similarly glycine is observed at P2, whereas serine was the most favorable residue in PS-SCL. This affinity for glycine at P4 and P2 may be a result of increased flexibility of the peptide resulting in an increased kinetic rate of cleavage for substrate phage. Similar results were observed when substrate phage display was performed on both tissue-type plasminogen activator and uPA (32).

One intriguing finding from the substrate phage display (Table I) was the apparent dependence between P4 and P3. If P3 is basic, then P4 tends to be non-basic (15 of 17 clones). Similarly, if P4 is basic, then P3 tends to be non-basic (13 of 15 clones). Thus on average, basic residues are most abundant at

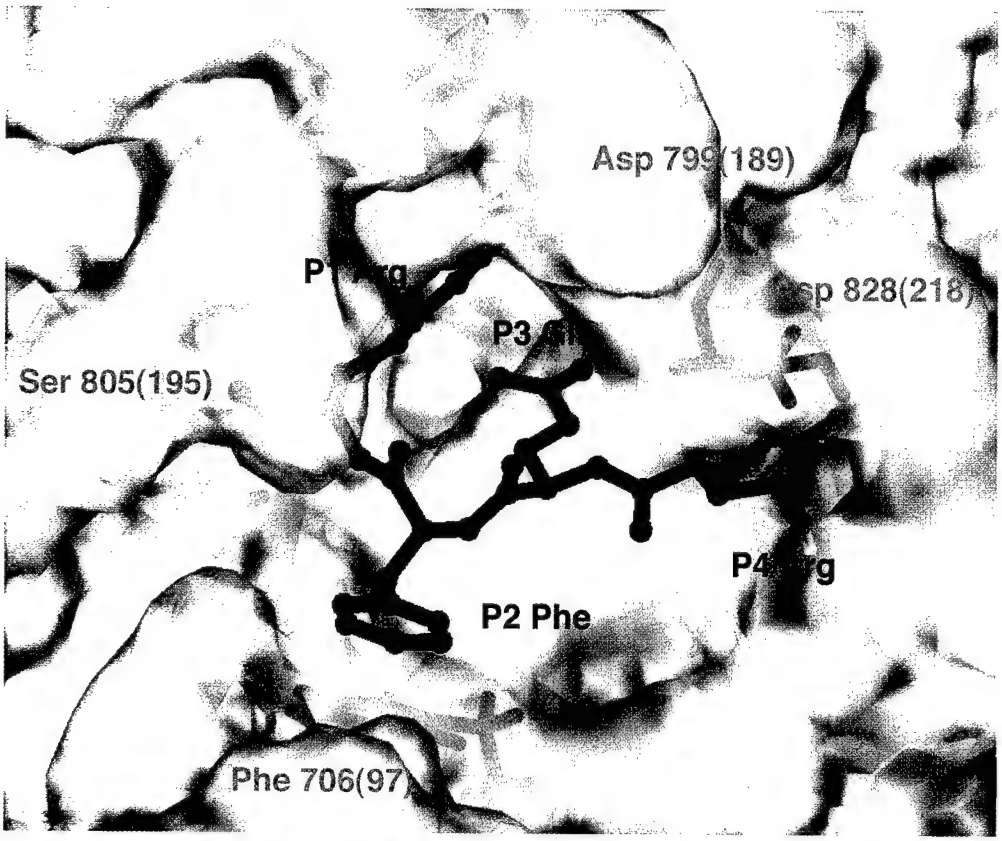

FIG. 5. **The active site from a model of MT-SP1 is shown with the substrate Arg-Phe-Gln-Arg bound in the S1–S4 subsites, respectively.** MT-SP1 side chains are shown in *red*, and the substrate is shown in *blue*. The protease amino acids are labeled with MT-SP1 numbering and chymotrypsinogen numbering in *parentheses*.

both P3 and P4, but for each individual cleavage sequence either P3 or P4 is basic but not both together. A second substrate phage display library was constructed to explore this possibility. The library was designed based upon the consensus sequence obtained from the PS-SCL. The P3 and P2 positions were fixed as a mixture of (Arg/Lys/Gln) and (Gly/Ala/Ser), respectively, whereas P4 was allowed to vary. Based upon the observations from the unbiased library, the expectation would be that if P3 is basic, then P4 should be predominantly occupied by neutral side chains. The results from this biased library are displayed in Table II and Fig. 4*B*. Indeed, since P3 is constrained to be a basic residue or glutamine, the predominant occupation of P4 is with a neutral residue, further verifying the observed dependence between P4 and P3.

To assist in defining the molecular determinants of substrate specificity, a homology model of MT-SP1 was constructed. The MT-SP1 amino acids were threaded onto the β-tryptase crystal structure (24) (Protein Data Bank code 1AOL). A substrate for MT-SP1 was modeled in the putative binding pocket using the active-site protease binding loop of ecotin that was derived from an ecotin-trypsin crystal structure (25).The S1 subsite specificity for basic amino acids can be attributed to the presence of aspartate 799 at the bottom of this S1 binding pocket. The S2 subsite is predicted to be a shallow groove; however, a Phe in the P2 position would be expected to make favorable interactions with Phe-706 of MT-SP1. Asp-828 of MT-SP1 could potentially form a salt bridge with either P4 or P3 depending on the conformation of the side chain, resulting in basic specificity in both P4 and P3. The active site from this MT-SP1 model complexed to a substrate Arg-Phe-Gln-Arg in P1 through P4, respectively, is displayed in Fig. 5.

Macromolecular Substrate Determination—Determinination of the substrate specificity of MT-SP1 may provide insight into the natural function of the enzyme. Information regarding the peptide substrate specificity combined with the knowledge of enzyme localization led to the testing of logical macromolecular substrates of MT-SP1 that are localized to the extracellular surface. Potential candidates for MT-SP1 cleavage are the protease-activated receptors (see Ref. 33 and references therein). PARs are activated by cleavage of a single site in their N-terminal exodomains. Of the four PARs known, only the cleavage site of PAR2 contains a basic residue in P4 (Ser) or P3 (Lys) and a small residue or phenylalanine in P2 (Gly). This led to the expectation that MT-SP1 would activate PAR2 but not activate PAR1, -3, and -4. The activation of these receptors was tested by injecting *Xenopus* oocytes with PAR cRNAs and monitoring activation of the receptors upon addition of exogenous protease. Addition of MT-SP1 catalytic domain to a final concentration of 1, 10, or 100 nM led to activation of mPAR2 and hPAR2 (data not shown) at 10 and 100 nM, and activation of hPAR1, -3, or -4 was not observed at any of the three concentrations (Fig. 6*A*). This specificity for PAR2 was seen even when PAR2 was expressed at much lower levels than PAR1, PAR3, or PAR4 (Fig. 6*B*). In addition to MT-SP1, 0.5 nM trypsin was also shown to activate PAR2. The PAR1, -3, and -4 receptors were functional, since these receptors were activated by thrombin. These data show that the MT-SP1 catalytic domain can selectively activate PAR2 over the other receptors, validating the substrate specificity determined by PS-SCL and phage display.

Another potential substrate that is consistent with the MT-SP1 specificity profile is single-chain urokinase-type plasminogen activator (sc-uPA). sc-uPA contains a neutral P4 (Pro) with a basic P3 (Arg), a Phe at P2, and a Lys at P1. The macromolecular substrate sc-uPA is a good test for the expected P2 Phe specificity. Indeed, sc-uPA is an excellent sub-

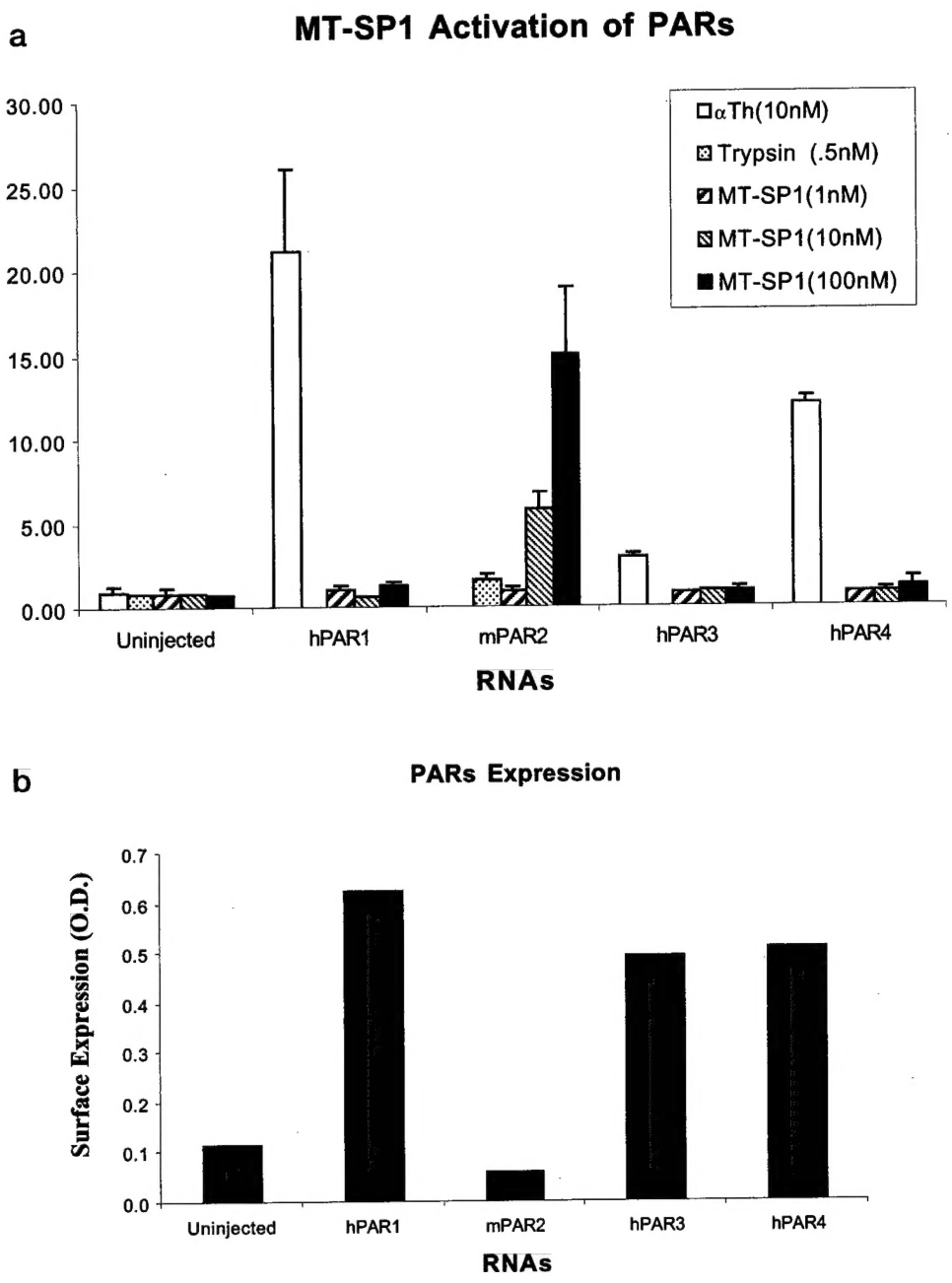

FIG. 6. **Activation of PAR2 by soluble MT-SP1 protease domain.** *a, Xenopus* oocytes were injected with cRNA encoding the indicated PAR, and protease-triggered ^{45}Ca release was assessed. Data shown are expressed as fold increase over basal (^{45}Ca released in the 10 min after agonist addition/^{45}Ca released in the 10 min before). *B,* surface expression of the PARs in *a* was determined by binding of a monoclonal antibody to a FLAG epitope displayed at the N terminus of each receptor. *a* and *b*, the data shown are means of duplicate determinations, and the results shown are representative of those obtained in three separate experiments.

strate for MT-SP1 as shown in Fig. 7. There is an increase in proteolytic activity that is dependent upon the presence of both sc-uPA and MT-SP1 that increases in time (Fig. 7). Concomitant with this increase in activity is cleavage of sc-uPA to the A- and B-chain components, as expected upon activation of the enzyme (Fig. 7). Under the same conditions, plasminogen was not activated by MT-SP1 (data not shown). Plasminogen has a small P2 residue (Gly) but lacks a basic P4 or P3 residue. These results further verify the specificity of MT-SP1 derived from the substrate libraries.

Plasmin has been shown to activate sc-uPA *in vitro* (34); this activation presumably would represent a feedback cycle where a small amount of active uPA would activate plasminogen to plasmin, and the resulting plasmin would activate sc-uPA. Other enzymes have also been reported to activate sc-uPA, including plasma kallikrein (35), cathepsin B (36), cathepsin L (37), mast cell tryptase (38), and prostate-specific antigen (39). In these studies, sc-uPA was activated using a substrate to enzyme ratio of 30:1, 10:1, 200:1, 50:1, and 10:1, respectively. Under similar conditions, MT-SP1 activates sc-uPA at a substrate:enzyme ratio of 5,000:1. These assays were performed with 1 nM MT-SP1, suggesting highly potent activation of sc-uPA (Fig. 7).

DISCUSSION

We previously reported the cloning and characterization of MT-SP1 derived from the cDNA of the PC-3 human prostatic carcinoma cell line (1). From the translation of the cDNA, MT-SP1 was predicted to be a type II transmembrane protein. A partial MT-SP1 cDNA had been reported by another labora-

TABLE I

Substrate specificity of MT-SP1 determined by substrate phage

The unbiased library has P1 fixed as R, whereas P4, P3, P2, and P1′ can encode any amino acid; sequences are shown from round 8.

Unbiased library clone number[a]	P4	P3	P2	P1	P1′
1	Val	Thr	Gly	Arg	Ser
2	Val	Arg	Gly	Arg	Ser
3	Ala	Gln	Gly	Arg	Met
4	Arg	Glu	Gly	Arg	Met
5	Arg	Glu	Gly	Arg	Thr
6	Gly	Ser	Gly	Arg	Trp
7		Gln	Gly	Arg	Arg
8	Gly	Gln	Gly	Arg	
9	Lys	Gln	Gly	Arg	Ala
10	Arg	Lys	Gly	Arg	Ser
11	Gly	Arg	Gly	Arg	
12	Gly	Lys	Gly	Arg	Thr
13	Glu	Arg	Gly	Arg	Ser
14	Ala	Arg	Gly	Arg	Arg
15	Lys	Met	Gly	Arg	Arg
16	Arg	Arg	Gly	Arg	Thr
17	Pro	Leu	Gly	Arg	Ser
18	Lys	Glu	Gly	Arg	Leu
19	Arg	Glu	Gly	Arg	Val
20	Arg	Met	Gly	Arg	Ala

TABLE II

Substrate specificity of MT-SP1 determined by substrate phage

The biased library has P3 fixed as (Arg/Lys/Gln), P2 fixed as (Ser/Ala/Gly), and P1 fixed as R, whereas P4, P1′, and P2′ can encode any amino acid sequences that are shown from round 5.

Biased library clone number[b]	P4	P3	P2	P1	P1′	P2′
1	Leu	Lys	Ser	Arg	Val	Lys
2	Ser	Lys	Ser	Arg	Thr	Leu
3	Phe	Gln	Cys	Arg	Val	Phe
4	Leu	Lys	Ser	Arg	Leu	Ser
5	Ser	Lys	Ser	Arg	Leu	Ser
6	Phe	Lys	Ala	Arg	Asn	Cys
7	His	Lys	Gly	Arg	Ala	Lys
8	Phe	Gln	Ser	Arg	Met	Glu
9	Ile	Arg	Ser	Arg	Tyr	Val
10	Tyr	Lys	Ser	Arg	Asn	Leu
11	Trp	Lys	Ser	Arg	Ser	Asn
12	Val	Lys	Ser	Arg	Thr	Ser
13	Val	Asn	Cys	Arg	Thr	Asn
14	Ser	Lys	Ala	Arg	Thr	Thr
15	Leu	Lys	Ser	Arg	Val	His
16	Ala	Gln	Ser	Arg	Met	Ser
17	Ile	Lys	Gly	Arg	Met	Ala
18	Asp	Gln	Ser	Arg	Met	Thr
19	Arg	Gln	Ser	Arg	Leu	Cys
20	Phe	Gln	Ser	Arg	Gly	Asn
21	Val	Lys	Ser	Arg	Leu	Cys

tory and referred to as "matriptase" (3). The matriptase cDNA lacks the 5′-coding region of the MT-SP1 cDNA, resulting in the truncation of the predicted signal anchor domain and, instead, is reported to contain a signal peptide. We report immunofluorescence and cell-surface biotinylation studies that show MT-SP1 protein is localized to the extracellular cell surface. Moreover, earlier work from the same laboratory that published the matriptase cDNA clone supports the extracellular surface localization (40). In that work, a protein that cross-reacts with matriptase antibodies shows extracellular localization on the surface of breast cancer cells using a cell-surface biotinylation assay and subcellular fractionation further localizes matriptase to the membrane. Their conclusion was that the protein that cross-reacts with matriptase antibodies is an integral membrane protein. Therefore, these data are consistent with the presence of a signal/anchor transmembrane domain in the translated MT-SP1 cDNA and are inconsistent with the presence of a signal peptide as suggested for the matriptase cDNA translation.

One possible explanation for the observed soluble forms of MT-SP1/matriptase protein is through shedding from the extracellular surface. For example, the protein sequenced for the matriptase clone was isolated from breast milk and not from the extracellular surface of cells (3). N-terminal amino acid sequencing showed sequence corresponding to amino acids 350–358 in the MT-SP1 protein translation and amino acids 228–236 in the matriptase translation, suggesting that the form of MT-SP1 isolated in breast milk most likely is cleaved from the extracellular surface and released into milk. These data, therefore, do not conflict with the proposed localization and protein translation for MT-SP1. Another possibility is that the matriptase clone is produced through alternative splicing, resulting in a soluble form of the protein. Isolation and N-terminal sequencing of the soluble forms may be necessary to differentiate between shed forms of the protein and secreted forms of the protein.

MT-SP1 protein has a predicted molecular mass of 95 kDa, and matriptase has a predicted size of 76 kDa. The previous

matriptase studies reported that the protein isolated from breast cancer cells is 80 kDa under non-reducing conditions (40, 41). MT-SP1 under non-reducing conditions has an apparent size of 80 kDa (Fig. 1, *4th lane*). However, deglycosylated and reduced MT-SP1 derived from PC-3 cells (Fig. 1, *6th lane*) has an apparent size of 87 kDa. Thus, there appears to be significant folding of the protein under non-reducing conditions, leading to a molecular weight that is smaller than the predicted molecular weight. *In vitro* transcription/translated product from the full-length MT-SP1 cDNA clone (Fig. 1, *7th lane*) also appears to be 87 kDa; therefore, the full-length protein may run slightly smaller than the expected 95 kDa.

In a previous paper, the matriptase cDNA clone was transfected into COS-7 cells. Membrane extracts of these cells were compared in an immunoblot to matriptase derived from the conditioned medium of T-47D human breast cancer cells (3). Presumably matriptase is cell-surface bound, similar to expression of MT-SP1 constructs lacking the signal/anchor domain. Under non-reducing conditions, the size of matriptase appears to be the same size as the protein isolated from the breast cancer cells; unfortunately, no molecular weight was designated in the figure, making it difficult to ascertain the size of the proteins. Since the matriptase from the breast cancer cell line was derived from the conditioned media and not from the cell surface, this protein may be cleaved from the surface of the cells or result from an alternatively spliced form of the protein, resulting in a molecular weight that corresponds to a size similar to the predicted matriptase protein (76 kDa).

There is strong sequence conservation between MT-SP1 and the mouse homolog epithin (2), which also has a predicted signal anchor domain. If the N-terminal transmembrane domain were untranslated, then divergence would be expected at both the cDNA and protein level. Instead, strong conservation of amino acids is observed in this N-terminal region, supporting the suggested protein translation and localization suggested for MT-SP1.

The results from PS-SCL implied that the most effective substrate would contain Lys-Arg-Ser-Arg in the P4 to P1 sites, respectively. However, since PS-SCL reveals the ideal amino acid for a given position on average, interdependences between positions are not apparent. However, the clones derived from substrate phage studies (Table I) revealed a striking trend; if P3 is basic, then P4 tends to be non-basic (15 of 17 clones); similarly, if P4 is basic, then P3 tends to be non-basic (13 of 15 clones). Thus on average, basic residues are the most abundant of the amino acids at P3 and P4, but for each individual sequence either P3 or P4 is basic but not both simultaneously. Taking the PS-SCL and the substrate phage together, the ideal sequence should be P4-(Arg/Lys)P3-(*X*)P2-(Ser)P1-(Arg)P1′-(Ala) and P4-(*X*)P3-(Arg/Lys)P2-(Ser)P1(Arg)P1′(Ala), where *X* must be a non-basic amino acid. Although insight into the function of the protease cannot be gained from this substrate specificity alone, the specificity can be used to identify possible macromolecular substrates, and these substrates can be tested *in vitro*.

Since MT-SP1 is localized to the extracellular surface of cells, logical substrates might have similar localization and should be cleaved/activated by proteases. This candidate approach revealed that PAR2 and sc-uPA were macromolecular substrates of MT-SP1. PAR2 is highly expressed in human pancreas, kidney, colon, liver, and small intestine and is expressed to a lower extent in the prostate, heart, lung, and trachea (42). In the small intestine, trypsin may be the physiological activator of PAR2; activation of PAR2 through trypsin cleavage may regulate the epithelium and mediate inflammation and cytoprotection (13). Trypsin may also activate PAR2 in the airways

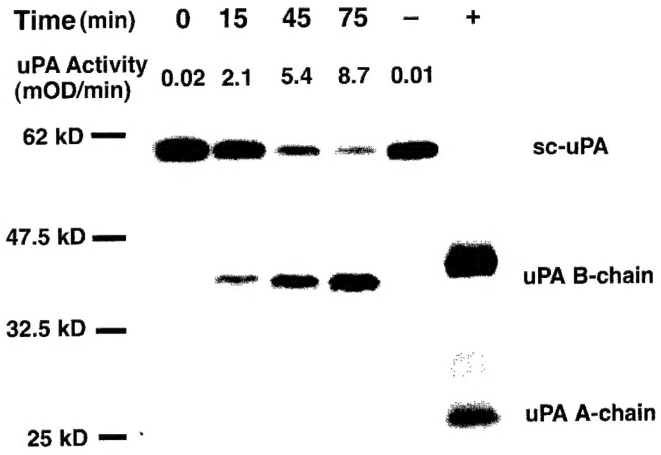

FIG. 7. **Activation of sc-uPA with MT-SP1.** Data from a representative experiment are shown. 5 μM uPA activation with 1 nM MT-SP1at 37 °C is assayed at specified times by removing aliquots and monitoring activity at 25 °C against the substrate Spectrozyme uK. Activity shown represents a 133-fold dilution from the original reaction mixture. Cleavage of 5 μM sc-uPA with 1 nM MT-SP1 at 37 °C is examined over time using immunoblot analysis. sc-uPA is cleaved into an A-chain and B-chain upon activation. Native, active uPA, which is used as a control (+), has different glycosylation compared with recombinant sc-uPA used in the assay, leading to differences in molecular weight. Unreacted sc-uPA incubated under the same conditions is shown in the – *lane*.

to initiate a bronchoprotective response (14).However, trypsin, most likely, is not the only physiological activator of PAR2, since trypsin is not coexpressed in all tissue types listed above. Another possible activator of PAR2 is mast cell tryptase, which has been shown to activate PAR2 in a tissue culture system (43). However, the cleavage of PAR2 by tryptase would require the presence of mast cells, which are usually involved in an inflammatory response; thus other activators of PAR2 may exist. MT-SP1 has a similar profile of tissue expression as PAR2 (1), and MT-SP1 and PAR2 are coexpressed in some cell types, including the prostate carcinoma cell line, PC-3 (1, 42). Furthermore, both proteins share the same extracellular surface localization, so it is possible that MT-SP1 may be a natural activator of PAR2.

sc-uPA is the other candidate that was activated by MT-SP1. Although the biology of PAR2 still is being elucidated, the biological roles of uPA are well established (see *e.g.* Refs. 17 and 18). For example, uPA has been implicated in tumor cell invasion and metastasis; cancer cell invasion into normal tissue can be facilitated by uPA through its activation of plasminogen, which degrades the basement membrane and extracellular matrix. Thus, activators of sc-uPA would be expected to increase invasiveness and possibly the metastatic capacity of tumor cells. The PC-3 prostate cancer cell line coexpresses MT-SP1 (1), uPA (44), and the uPA receptor by immunofluorescence,[3] allowing cell-surface localization of the protease. Thus, MT-SP1 may activate sc-uPA on the surface of PC-3 cells and thereby increase the invasiveness of these cells. Indeed, potent inhibitors of MT-SP1 inhibit the proliferation and metastasis of PC-3 cells in SCID mice.[4] However, further studies are being performed to identify clearly MT-SP1 as the selective target of the protease inhibitor. Nevertheless, the finding that MT-SP1 activates sc-uPA may have interesting implications for the role of proteolysis in cancer.

MT-SP1 is a highly active enzyme with k_{cat}/K_m for synthetic peptide substrate turnover approaching levels of the digestive

[3] T. Takeuchi, M. Shuman, and C. S. Craik, unpublished results.
[4] F. Elfman, T. Takeuchi, M. Conn, C. S. Craik, and M. Shuman, unpublished results.

enzyme trypsin (1). However, MT-SP1 is not a nonspecific degradative enzyme. The specificity of MT-SP1 for macromolecular substrates closely matches the specificity determined in PS-SCL and substrate phage display. Thus, although PAR2 is activated, the highly similar PAR1, -3, and -4 are not activated. The substrate sc-uPA is activated, but the plasminogen is not cleaved even at much higher concentrations of MT-SP1. Interestingly, the activation site of pro-MT-SP1 matches the substrate specificity determined for the active enzyme, and recombinant MT-SP1 was found to autoactivate upon removal of denaturant (1). The high activity of the MT-SP1 catalytic domain may allow residual activity of the pro-enzyme, allowing autoactivation to occur. Thus, MT-SP1 could autoactivate and initiate signaling and proteolytic cascades via activation of PAR2 or sc-uPA. Other membrane-type serine proteases involved in proteolytic cascades are enteropeptidase (4), which activates trypsinogen in the gut for digestion, and hepsin (46), which has been shown to activate factor VIIa in a blood coagulation cascade (47). Other membrane-type serine proteases include TMPRSS2 (48), human airway trypsin-like protease (49), and corin (50). Membrane-type serine proteases as signaling molecules that play key regulatory roles may become more prevalent as these novel proteases are further characterized.

Acknowledgments—We thank Bradley Backes, Francesco Leonetti, and Jonathan Ellman for PS-SCL library synthesis and Ibrahim Adiguzel, Yonchu Jenkins, and Sushma Selvarajan for technical assistance and helpful discussions.

REFERENCES

1. Takeuchi, T., Shuman, M. A., and Craik, C. S. (1999) *Proc. Natl. Acad. Sci. U. S. A.* **96,** 11054–11061
2. Kim, M. G., Chen, C., Lyu, M. S., Cho, E.-G., Park, D., Kozak, C., and Schwartz, R. H. (1999) *Immunogenetics* **49,** 420–428
3. Lin, C.-Y., Anders, J., Johnson, M., Sang, Q. A., and Dickson, R. B. (1999) *J. Biol. Chem.* **274,** 18231–18236
4. Huber, R., and Bode, W. (1978) *Acc. Chem. Res.* **11,** 114–122
5. Pinilla, C., Appel, J. R., Blanc, P., and Houghten, R. A.(1992) *BioTechniques* **13,** 901–905
6. Rano, T. A., Timkey, T., Peterson, E. P., Rotonda, J., Nicholson, D. W., Becker, J. W., Chapman, K. T., Thornberry, N. A. (1997) *Chem. Biol.* **4,** 149–155
7. Thornberry, N. A., Rano, T. A., Peterson, E. P., Rasper, D. M., Timkey, T., Garcia-Calvo, M., Houtzager, V. M., Nordstrom, P. A., Roy, S., Vaillancourt, J. P., Chapman, K., T., and Nicholson, D. W. (1997) *J. Biol. Chem.* **272,** 17907–17911
8. Harris, J. L., Peterson, E. P., Hudig, D., Thornberry, N. A., and Craik, C. S. (1998) *J. Biol. Chem.* **273,** 27364–27373
9. Matthews, D. J., and Wells, J. A. (1993) *Science* **260,** 1113–1117
10. Matthews, D. J., Goodman, L. J., Gorman, C. M., and Wells, J. A. (1994) *Protein Sci.* **3,** 1197–1205
11. Schecter, I., and Berger, A. (1967) *Biochem. Biophys. Res. Commun.* **27,** 157–162
12. Backes, B. J., Harris, J. L., Leonetti, F., Craik, C. S., and Ellman, J. A. (2000) *Nat. Biotechnol.* **18,** 187–193
13. Kong, W., McConalogue, K., Khitin, L. M., Hollengerg, M. D., Payan, D. G., Bohm, S. K., and Bunnett, N. W. (1997) *Proc. Natl. Acad. Sci. U. S. A.* **94,** 8884–8889
14. Steinhoff, M., Vergnolle, N., Young, S. H., Tognetto, M., Amadesi, S., Ennes, S. H., Trevisani, M., Hollenberg, M. D., Wallace, J. L., Caughey, G. H., Mitchell, S. E., Williams, L. M., Geppetti, P., Mayer, E. A., Bunnett, N. W. (2000) *Nat. Med.* **6,** 151–158
15. Cocks, T. M., Fong, B., Chow, J. M., Anderson, G. P., Frauman, A. G., Goldie, R. G., Henry, P. J., Carr, M. J., Hamilton, J. R., and Moffatt, J. D. (1999) *Nature* **398,** 156–160
16. Miyata, S., Koshikawa, N., Yasumitsu, H., and Miyazaki, K. (2000) *J. Biol. Chem.* **275,** 4592–4598
17. Dano, K. Andreasen, P. A., Grondahl-Hansen, J., Kristensen, P., Nielsen, L. S., and Skriver, L. (1985) *Adv. Cancer Res.* **44,** 139 266
18. Andreasen, P. A., Kjoller, L., Christensen, L., and Duffy, M. J. (1997) *Int. J. Cancer* **72,** 1–22
19. Unal, A., Pray, T. R., Lagunoff, M., Pennington, M. W., Ganem, D., and Craik, C. S. (1997) *J. Virol.* **71,** 7030–7038
20. Weis, K., Dingwall, C., and Lamond, A. I. (1996) *EMBO J.* **15,** 7120–7128
21. Altin, J. G., and Pagler, E. B. (1995) *Anal. Biochem.* **224,** 382–389
22. Backes, B. J., and Ellman, J. A. (1999) *J. Org. Chem.* **64,** 2322–2330
23. Ostresh, J. M., Winkle, J. H., Hamashin, V. T., and Houghten, R. A. (1994) *Biopolymers* **34,** 1681–1689
24. Pereira, P. J., Bergner, A., Macedo-Ribeiro, S., Huber, R., Matschiner, G., Fritz, H., Sommerhoff, C. P., and Bode, W. (1998) *Nature* **392,** 306–311
25. McGrath, M. E., Erpel, T., Bystroff, C., and Fletterick, R. J. (1994) *EMBO J.* **13,** 1503–1507
26. Vu, T.-K. H., Hung, D. T., Wheaton, V. I., and Coughlin, S. R. (1991) *Cell* **64,** 1057–1068
27. Nystedt, S., Larsson, A. K., Aberg, H., and Sundelin, J. (1995) *J. Biol. Chem.* **270,** 5950–5955
28. Ishihara, H., Connolly, A. J., Zeng, D., Kahn, M. L., Zheng, Y. W., Timmons, C., Tram, T., and Coughlin, S. R. (1997) *Nature* **386,** 502–506
29. Kahn, M. L., Zheng, Y. W., Huang, W., Bigornia, V., Zeng, D., Moff, S., Farese, R. V., Jr, Tam, C., and Coughlin, S. R. (1998) *Nature* **394,** 690–694
30. Ishii, K., Hein, L., Kobilka, B. K., and Coughlin, S. R. (1993) *J. Biol. Chem.* **268,** 9780–9786
31. Schuberth, H.-J., Kroell, A., and Leibold, W. (1996) *J. Immunol. Methods* **189,** 89–98
32. Ke, S.-H., Coombs, G. S., Tachias, K., Navre, M., Corey, D. R., and Madison, E. L. (1997) *J. Biol. Chem.* **272,** 16603–16609
33. Coughlin, S. R. (1999) *Proc. Natl. Acad. Sci. U. S. A.* **96,** 11023–11027
34. Nielsen, L. S., Hansen. J. G., Skriver, L., Wilson, E. L., Kaltoft, K., Zeuthen, J., and Dano, K. (1982) *Biochemistry* **1982,** 6410–6415
35. Ichinose, A., Fujikawa, K., and Suyama, T. (1986) *J. Biol. Chem.* **261,** 3486–3489
36. Kobayashi, H., Schmitt, M., Goretzki, L., Chucholowski, N., Calvete, J., Kramer, M., Gunzler, W. A., Janicke, F., and Graeff, H. (1991) *J. Biol. Chem.* **266,** 5147–5152
37. Goretzki, L., Schmitt, M., Mann, K., Calvete, J., Chucholowski, N., Kramer, M., Gunzler, W. A., Janicke, F., and Graeff, H. (1992) *FEBS Lett.* **297,** 112–118
38. Stack, M. S., and Johnson, D. A. (1994) *J. Biol. Chem.* **269,** 9416–9419
39. Yoshida, E., Ohmura, S., Sugiki, M., Maruyama, M., and Mihara, H. (1995) *Int. J. Cancer* **63,** 863–865
40. Lin, C.-Y., Wang, J.-K., Torri, J., Dou, L., Sang, Q. A., and Dickson, R. B. (1997) *J. Biol. Chem.* **272,** 9147–9152
41. Shi, Y. E., Torri, J., Yieh, L., Wellstein, A., Lippman, M. E., and Dickson, R. B. (1993) *Cancer Res.* **53,** 1409–1415
42. Bohm, S. K., Kong, W., Bromme, D., Smeekens, S. P., Anderson, D. C., Connolly, A., Kah, M., Nelken, N. A., Coughlin, S. R., Payan, D. G., and Bunnett, N. W. (1996) *Biochem. J.* **314,** 1009–1016
43. Molino, M., Barnathan, E. S., Numerof, R., Clark, J., Dreyer, M., Cumashi, A., Hoxie, J. A., Schechter, N., Woolkalis, M., and Brass, L. F. (1997) *J. Biol. Chem.* **272,** 4043–4049
44. Yoshida, E., Verrusio, E. N., Mihara, H., Oh, D., and Kwaan, H. C. (1994) *Cancer Res.* **54,** 3300–3304
45. Perona, J. J., and Craik, C. S. (1997) *J. Biol. Chem.* **272,** 29987–29990
46. Leytus, S. P., Loeb, K. R., Hagen, F. S., Kurachi, K., and Davie, E. W. (1988) *Biochemistry* **27,** 1067–1074
47. Kazama, Y., Hamamoto, T., Foster, D. C., and Kisiel, W. (1995) *J. Biol. Chem.* **270,** 66–72
48. Poloni-Giacobino, A., Chen, H., Peitsch, M. C., Rossier, C., and Antonarkis, S. E. (1997) *Genomics* **44,** 309–320
49. Yamakoka, K., Masuda, K., Ogawa, H., Takagi, K., Umemoto, N., and Yasuoka, S. (1998) *J. Biol. Chem.* **273,** 11895–11901
50. Yan, W., Sheng, N., Seto, M., Morser, J., and Wu, Q. (1999) *J. Biol. Chem.* **274,** 14926–14935
51. Bork, P. and Beckmann, G. (1993) *J. Mol. Biol.* **231,** 539–545
52. Krieger, M., and Herz, J. (1994) *Annu. Rev. Biochem.* **63,** 601–637